UNIVERSITÀ
DEGLI STUDI
DI PADOVA

Dipartimento di Medicina (DIMED)

INTERNATIONAL PhD PROGRAM IN:

ARTERIAL HYPERTENSION AND VASCULAR BIOLOGY

CYCLE XXIX

Molecular Characterization of A Novel Mutation In The Renal NaCl Cotransporter Causing Gitelman's Syndrome By Impairing Transporter Trafficking

Coordinatore: Ch.mo Prof. Gian Paolo Rossi

Supervisore: Ch.mo Prof. Gian Paolo Rossi

Dottoranda: Verdiana Ravarotto

Academic Year: 2015/2016

«Dubium sapientiae initium»

(Doubt is the beginning of wisdom)

René Descartes, Meditationes de prima philosophia

CONTENTS

RIASSUNTO

Le mutazioni che colpiscono il cotrasportatore per il sodio e cloro (NCC) nel tubulo contorto distale del nefrone, sono responsabili della sindrome di Gitelman (GS). Quest'ultima è una rara tubulopatia renale autosomica recessiva caratterizzata da alterazioni elettrolitiche simili a quelle indotte dal trattamento ad alte dosi con diuretici tiazidici. La co-presenza di ipomagnesemia e ipocalciuria è una delle caratteristiche di GS che la distinguono da un'altra tubulopatia renale ipokalemica, la sindorme di Bartter (BS). Generalmente, i soggetti affetti sono eterozigoti composti con una prevalenza stimata di 1 su 40000. La malattia può essere silente per anni prima di presentarsi nell'età adulta. Riconoscerne la componente genetica è fondamentale per lo screening e la diagnosi. Recenti studi hanno di fatto dimostrato come le mutazioni a carico dei regolatori renali dell'omeostasi del sodio siano sottostimate nella popolazione generale.

Nel nostro database universitario di pazienti BS/GS abbiamo riscontrato una nuova mutazione puntiforme (c.1204G>A che comporta lo scambio aminoacidico Gly394Asp) nel cotrasportatore del sodio e cloro NCC (SLC12A3) in una giovane donna con ipokaliemia, ipomagnesemia e ipocalciuria associati a dolori e crampi muscolari. Il presente studio ha lo scopo di investigare tramite un approccio biologico molecolare come questa mutazione influenzi la funzionalità di NCC.

Previo screening con softwares bioinformatici che predicono la possibile patogenicità della mutazione, sono stati creati dei vettori di espressione contenenti le sequenze per NCC wild type e per NCC con mutazione G394D. Successivamente, le sequenze sono state trasfettate in una linea di cellule fetali umane ricombinate (HEK293) e in ovociti derivati da rane Xenopus Laevis. Nelle cellule trasfettate, l'immunoblotting di NCC wild-type ha dimostrato la presenza di due bande approssimativamente a 130 KDa e 115 KDa che corrispondono rispettivamente alla forma glicosilata e nativa della proteina. Al contrario, G394D-NCC presenta una sola banda a 115 KDa. Risultati simili sono stati ottenuti negli ovociti. In questi ultimi l'immunoistochimica ha inoltre mostrato una forte localizzazione di NCC wild-type presso la membrana, mentre NCC mutato rimane in compartimenti cellulari interni. Gli studi funzionali di uptake del sodio radioattivo ($^{22}Na^{+}$) hanno ulteriormente confermato che solo la proteina wild-type è in grado di riassorbire il sodio al contrario di G394D-NCC.

I risultati di questo studio dimostrano come la nuova mutazione puntiforme inibisca la funzione di NCC a causa della diminuita capacità della proteina di raggiungere la superficie cellulare. L'assenza di una forma glicosilata matura di G394D-NCC suggerisce che la mutazione ne condizioni il folding e ne provochi la ritenzione nel reticolo endoplasmico ove vengo attivati processi di degradazione anticipata.

SUMMARY

Mutations affecting the sodium-chloride cotransporter (NCC) in the distal convoluted tubule of the nephron are causative of Gitelman's syndrome (GS), a rare autosomal recessive disease characterized by electrolytic alterations similar to those induced by high dose thiazide treatment. Notably, the co-existence of hypomagnesemia and hypocalciuria is a feature of GS which is a distinguish hallmark from another hypokalemic renal tubulopathy, the Bartter's syndrome (BS). Commonly GS is heterozygous compound with an estimated prevalence of 1:40000 and can be silent for years before the revealing in the early adulthood. Recognizing the genetic background is fundamental for the screening and the diagnosis of the disease, as recently studies showed that mutation affecting regulators of renal salt handling are underestimated in the general population.

In a registry of BS/GS based at our University we discovered a novel point mutation (c.1204G>A which codify for an amino acid exchange G394D) in the sodium-chloride cotransporter NCC (SLC12A3) in a young woman with hypokalemia, hypomagnesemia and hypocalciuria associated to muscle pain and cramps. The present study aimed to investigate how this mutation affects NCC function by using a molecular biology approach and providing functional evidences.

After a prior screening with bioinformatics tools predicting the possible pathogenicity of the mutation, were created different expression vectors with either the wild-type (wt-NCC) or the mutated G394D-NCC sequences. DNA and in-vitro transcribed RNA were afterwards transfected in a human embryonic kidney cells line (HEK293) and injected into oocytes deriving from Xenopus Laevis frog respectively. In transfected HEK 293 cells, wildtype NCC was detected by immunoblotting as two bands at approximately 130 kDa and 115 kDa corresponding to fully and core-glycosylated NCC, respectively. In contrast, G394D-NCC was seen as a single band at about 115 kDa only, suggesting an impaired maturation of the mutated protein. Similar findings were made in the oocyte expression system. Confocal microscopy on the oocytes, did also show a strong cell surface localization of wildtype NCC while mutated NCC was retained at intracellular compartments. Consistently, a decent thiazide-sensitive $^{22}Na^{+}$ uptake into injected oocytes was only found for wildtype but not mutated NCC.

Taken together all the findings in this study, a novel GS point mutation has been characterized to diminish NCC function by impairing trafficking of the protein to the cell surface. The absence of any mature glycosylation form of G394D-NCC suggests that the mutation impairs protein folding leading to a retention of NCC in the endoplasmic reticulum.

INTRODUCTION

Gitelman's syndrome (GS, OMIM no. 263800) is an inherited autosomal recessive renal tubular disorder that affects sodium-chloride cotransporter (NCC) in the distal convoluted tubule (DCT) of the nephron. After its first description in 1966, GS was found to be far more uncommon then initially held. In fact, its estimated prevalence is about 1:40000, and the heterozygotes carriers involves about 1% in Caucasian populations. Thus GS is one of the most frequently inherited renal tubular disorders (1). The clinical features of GS usually manifest in adolescence or early adulthood, and entail muscle weakness, fatigue, joint pain, cramps and tetany (2). Its biochemical hallmarks comprise hypokalemia, metabolic alkalosis, sodium wasting, co-existence of hypomagnesemia and hypocalciuria, and normal or low blood pressure values, the latter occurring despite a prominent activation of the renin-angiotensin-aldosterone system (RAAS) (3). The molecular basis of GS was attributed to mutations of the solute carrier family 12 member 3 gene SLC12A3 gene, which cause loss-of-function of the NCC in the distal convoluted-tubule with renal sodium wasting triggering adaptive mechanisms in the kidney, including aldosterone-driven increased excretion of K^+ in exchange for Na^+.

Of note, the biochemical abnormalities of GS are reproduced pharmacologically by administration of thiazide diuretics which inhibit the NCC activity causing sodium and potassium wasting, hypovolemia, and RAAS activation. Thus, patients chronically treated with these agents can be regarded as the counterpart of the naturally occurring GS. Owing to their pathophysiologic consequences, GS mutations might blunt the hypertension phenotype in essential hypertensive patients, which conceivably led to underestimate the prevalence of GS mutations inasmuch the syndrome is usually sought for only in patients with hypotension. Indeed, a screening of 2492 members of the Framingham Heart Study (FHS) for variation in three genes causing Bartter's syndromes and variation in SLC12A3 gene, allowed the detection of 138 coding sequence variants. Those carrying the mutations had significantly lower age- and sex-adjusted systolic and diastolic BP compared to the non-carriers (4). While supporting the concept that alleles that alter renal salt handling affect BP variation in the general population, these results suggest that genetic testing for these syndromes could become part of the assessment of patients with BP disorders in the future.

The cloning and characterization of the SLC12A3 gene encoding the NCC unveiled several mutations affecting the whole protein gene occur in GS and leading to dysfunction of the cotransporter (5,6). To date, more then 180 mutations in SLC12A3 are found in the HGMD database (www.hgmd.cf.ac.uk), including missense, nonsense, frame-shift and splice site. Notwithstanding the large number of mutations, the molecular mechanisms whereby they impair the function of the NCC still remains unclear in most cases as most of the mutations were not functionally characterized. The described mutations are in the literature as affecting the cotransporter activity (by impairing synthesis of the protein), the trafficking of the cotransporter to the cell surface, the function of the protein itself at the cell surface, and finally by enhancing the degradation of the protein. According to some studies the central domain of NCC would determine ion translocation and confer thiazide-binding specificity, which could account for the pathogenic role of these missense mutations (7).

The syndrome was first described in 1966 when Gitelman reported the clinical case of two sisters who presented muscle weakness and had suffered for many years from a chronic dermatitis characterized by thickening with a purple-red hue that could have been related to magnesium deficiency (2,8,9). Successively Spencer and Voyce reported four siblings of another family: two of them had hypokalemia, hypomagnesaemia and decreased urinary calcium output with episodes of tetany, while other members were normal (10). The concept of "familial hypokalemia and hypomagnesemia disorder" due to nonspecific illness had more reports after its first description with a growing of symptoms. In 1992 Zagarra et al described a 33-year-old woman who presented with hypokalemia-hypomagnesemia associated with renal potassium and magnesium wasting (11). She had normal plasma calcium and normal serum calcitriol and parathyroid hormone. Moreover, a test with intravenous furosemide (a loop diuretic) evidenced abolition of hypocalciuria, but exaggerated natriuresis and magnesium excretion. The dissociation of renal calcium transport from magnesium transport, together with sodium wasting, suggested the presence of a defect in the distal tubule rather than in the loop of Henle. Furthermore, the patient had episodes of tetany and muscle cramps consistently with the syndrome of renotubular hypomagnesemia-hypokalemia with hypocalciuria, at that time already known as Gitelman's syndrome (GS) (11). For many years it remained challenging to discriminate Gitelman's from Bartter's syndrome (BS), which was previously described by Bartter et al in 1962 as hypokalemic alkalosis, aldosteronism, hyper/normocalciuria

disorder (12-14). Considering the phenotype, the two syndromes share similar features, except for the co-existence in GS of hypokalemia, hypomagnesemia and hypocalciuria. Moreover, subjects affected by GS have a prolongation of the QT interval on electrocardiogram and episodes of calcium pyrophosphate crystal deposition or chondrocalcinosis (13,15,16).

The onset time for the symptoms come in adulthood, or adolescence in some cases, while BS has a neonatal form, or classically appears in childhood (14,17). Clinically, GS has electrolyte abnormalities similar to those induced by treatment with Thiazide diuretics or other drugs that inhibit the Na-Cl cotransporter in the distal convoluted tubule (DCT) of the kidney. In 1996 Simon et al. were describing and characterizing some cotransporters and channels involved in the reabsorption of electrolytes to better gain insight in hypertension etiology (17-19). Assembling together the findings that in GS the reabsorption of the sodium and chloride occurred in the distal convoluted tubule in spite of the loop of Henle, and the concurrent hypomagnesemia and electrolytic impairment caused by thiazide treatment, Simon et al. could demonstrate a linkage between GS and the sodium-chloride cotransporter (NCC) (20). They identified a great amount of variants in the SLC12A3 gene, encoding for the NCC, which were of loss-of-function alleles. The genetic component in this syndrome is intriguing. It is known to be a rare autosomal recessive disease with a prevalence of 1:40000 with heterozygous compound, resulting in the most common frequent inherited renal tubular disorder. It is listed in the Mendelian Inheritance in Men (OMIM) with the number 268300 (http://omim.org/entry/263800) (1,18).

In heterozygous condition one of the two alleles present a mutation and the subject is a carrier non symptomatic. In homozygous both alleles are presenting the same mutation in the same loci and the subject is presenting the disease. In the *heterozygous compound* both alleles are affected by two different mutations in distinct loci (21). As clinical outcome, it can arise a milder form of the disease [Figure1].

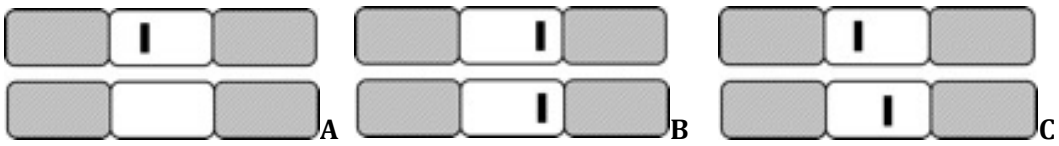

FIGURE1: Schematic representation of autosomes. Boxes indicate alleles, black rectangles indicate mutations. **A** Heterozygous genotype **B** Homozygous genotype **C** Homozygous compound genotype

Additionally, GS differs from BS for the genetic trait. While GS is identified as a monogenic disease due to mutations affecting NCC, BS is usually classified in 5 types regarding the protein affected with an earlier onset timing. The electrolyte abnormalities of BS are similar to those induced by treatment with furosemide or other loop diuretics that inhibit the Na-K-2Cl (NKCC2) cotransporter of the thick ascending limb of Henle's loop (TAL). Typically, NKCC2 mutations classify BS type I. Other mutations are found in genes involved in the regulation of NKCC2 activity, in particular, alterations in the apical ATP-sensitive K channel (renal outer medullary channel, ROMK) arise BS type II; mutations in the chloride channel Kb (ClCNKb) identify BS type III and furthermore, its regulatory protein Barttin can also be affected causing BS type IV. Type V BS is induced by mutations in the Ca^{2+} sensing receptor (CaSR) (14,17-19). [Figure2]

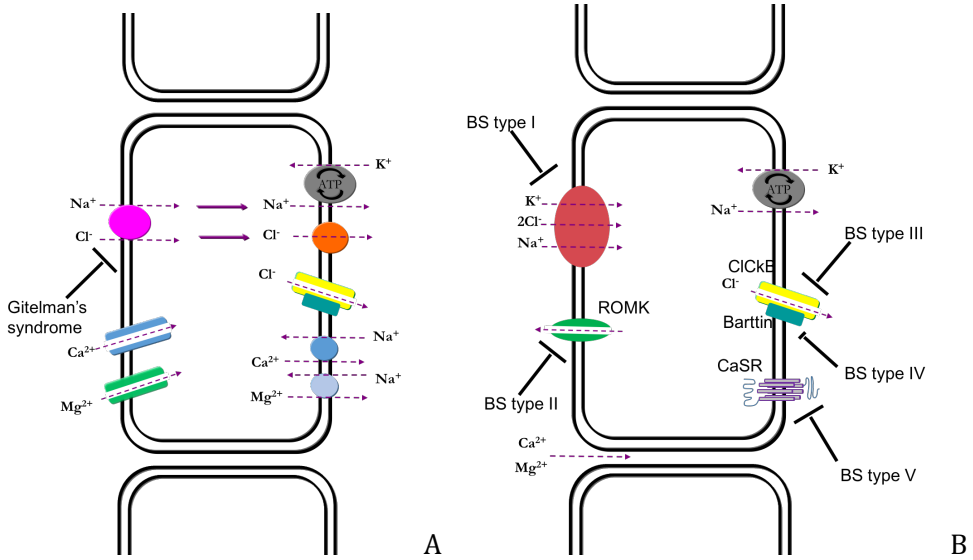

FIGURE 2: A Distal convoluted cells in Gitelman's syndrome. Mutations affect the Na-Cl cotransporters. **B** Thick ascending limb cells in Bartter's syndrome. Mutations affect different cotransporters or channels identifying different types.

Recently, a novel form of Bartter syndrome has also been described by Laghmani et al. as a transient antenatal form with polyhydramnios and mutations in the MAGED2 which encodes melanoma- associated antigen D2 (22).

Both GS and BS syndromes are characterized by marked RAAS stimulation featuring high plasma renin, angiotensin II (Ang II) and aldosterone. Notwithstanding this activation, patients show reduced peripheral resistance and normal to low blood pressure, along with resistance to the pressor effect of vasoconstrictors as Ang II and

norepinephrine (23). Hence it has been speculated, that heterozygous carriers of NCC mutation are partially protected from hypertension (4,24).

ANGIOTENSIN II SIGNALING IN GITELMAN'S SYNDROME

Studies in GS and BS may provide useful insights on understanding the mechanisms involved in the control and regulation of vascular tone and blood pressure in humans. In physiological conditions, Ang II is directly involved in activating microvascular signaling leading to increased peripheral resistance and hypertension. Of note, Calò et al. demonstrated that GS and BS patients have a blunted signaling of Ang II despite higher levels of the hormone and normal Ang II receptors number and affinity (23). This suggests that the Ang II signaling is interrupted at the post receptor level or very close to the central switch controlling Ang II signals. Due to their characteristic activation of RAAS with concomitant low blood pressure, the two syndromes can be viewed as ''mirror image'' of hypertension and as human model of endogenous antagonism of Ang II signaling via AT1R [Table 1].

Ang II short and long term signaling effects	BS/GS	Hypertension
Intracellular Ca^{2+} release	↓	↑
Intracellular IP_3 level	↓	↑
PKC expression and activity	↓	↑
NO system	↑	↓
ecNOS expression	↑	↓
NO dependent relaxation	↑	↓
$G_{\alpha q}$ expression	↓	↑
RGS-2 expression	↑	↓
Rho kinase expression/activity	↓	↑
Oxidative stress	↓	↑
Inflammatory state	↓	↑
Insulin resistance	↓	↑
Cardiovascular-renal target organ damage	Lack	Present

TABLE 1: Opposite effects of Angiotensin II signaling in BS/GS and in Hypertension. In hypertensive conditions, AngII signaling through AT1R promotes oxidative stress-related pathways, whereas in BS/GS the binding of AngII with AT2R induces favorable anti-

remodeling and anti-proliferative effects. Adapted from Ravarotto et al. High Blood Press Cardiovasc Prev (2015) 22:215

The multiple effects of Ang II function involve short or long-term signaling. The short-term signaling pathways are mediated by monomeric and heterotrimeric G proteins and phospholipase Cb (PLCβ). The bind of Ang II to its receptor AT1 promote the release of intracellular messengers inositol triphosphate (IP3) and Ca^{2+}, generation of superoxide and activation of protein kinase C (PKC) with ensuing vascular smooth muscle contraction (8). A counterbalancing system is represented by the nitric oxide (NO) system, which has vasodilatory and antiproliferative activity. NO is released by endothelial NO synthase (eNOS) and is negatively regulated by PKC. Therefore, the effect of Ang II on vascular function and structure is the result of the net balance of signaling molecules, oxidative stress and gasomessengers as nitric oxide (25,26).

The long-term effects of Ang II promote proliferation and cardiovascular-renal remodeling mostly through the induction of oxidative stress (27,28). The complex of Ang II with the AT1 G-protein-coupled receptors promotes alongside the increase of free intracellular Ca^{2+}, the activation of the RhoA/ Rho kinase pathway with subsequent vasoconstriction and insulin resistance (5). [Figure 3]

In hypertension Gq and Gi proteins mediate the activation of the PLC. The Ang II-AT1R complex couples with PLCb and promotes activation of PKC and phosphorylation of the regulatory chain of myosin II. In addition, the activation of the monomeric G-protein RhoA and its effector Rho kinase modulates the phosphorylation state of the regulatory chain of myosin II, mainly through inhibition of the myosin phosphatase target protein-1 (MYPT-1). These pathways induce vasoconstriction and increased peripheral resistance, while at the same time NO pathway is reduced (23).

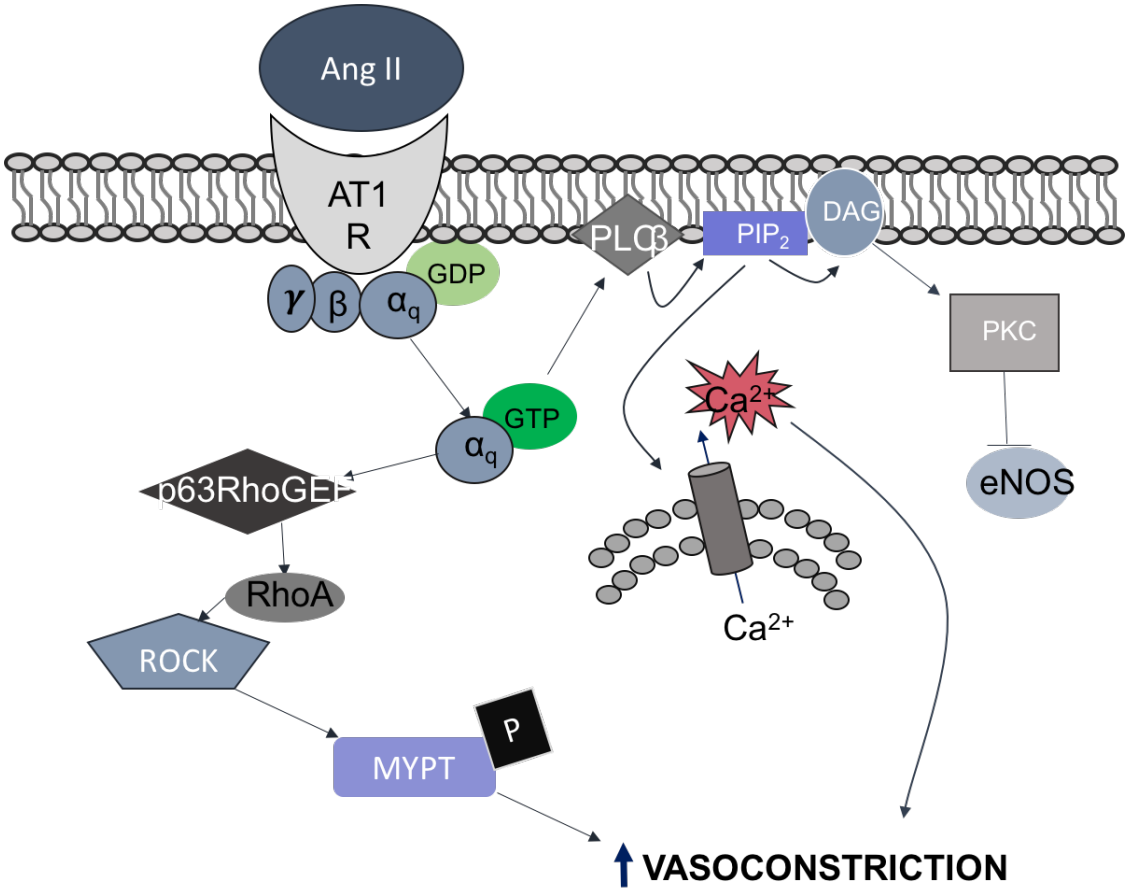

FIGURE 3: Schematic representation of Ang II signaling pathways involved in hypertension and complications (changes of cardiovascular structure: remodeling and atherogenesis; hypertension-inflammation relationship; hypertension-glucose transport and insulin resistance and sensitivity interrelationships). Ang II, angiotensin II; AT1-R, angiotensin II type 1 receptor; [beta] and [gamma] subunit of Gq protein; DAG, diacylglycerol; eNOS, endothelial subunit of nitric oxide synthase; PIP_2, inositol triphosphate; PKC, protein kinase C; PLC[beta], phospholipase C [beta]; RhoGEF, Rho guanine nucleotide exchange factor; ROCK, Rho Kinase; MYPT, myosin light chain target subunit-1. Adapted from Calò et al. J. Hypertens 32(11):2109-2119, November 2014 (23)

Ang II signaling in GS and BS is reversed: subjects affected have decreased gene and protein expression of the α subunit of Gq protein and blunted downstream intracellular events that promote Ca^{2+} release and PKC activation in the short-term pathway of Ang II (29,30) In addition, in these patients the evaluation of the NO system via the endothelial nitric oxide synthase (eNOS) mRNA levels, urinary excretion of NO metabolites and NO mediated vasodilation showed a significant increase of eNOS expression, and an increased NO mediated vasodilation compared with hypertensive patients (31-33).

The long-term network for GS and BS is characterized by underexpression of pro-oxidant elements, in favor of an antioxidant potential which is demonstrated by the augmented expression of heme oxygenase 1 (HO-1) and NOX4 and reduced $p22^{phox}$ (34,35) [Figure 4]

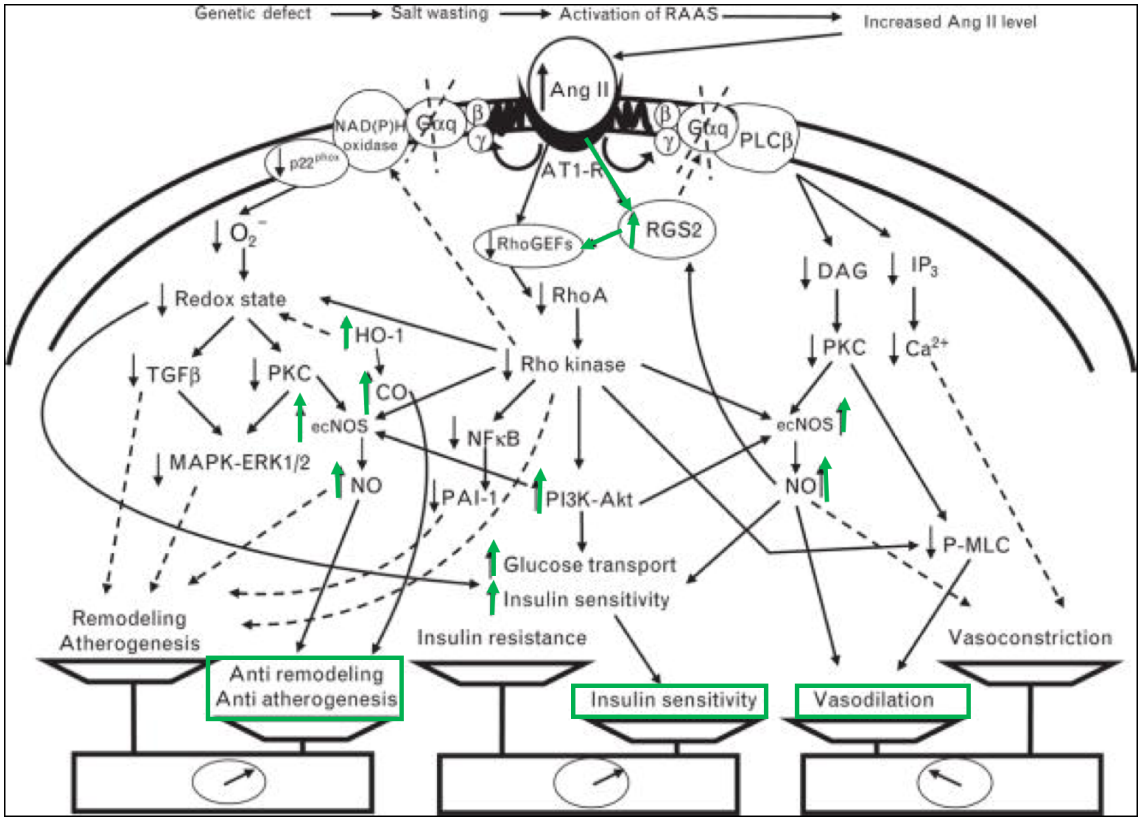

FIGURE 4: Ang II signaling and its relationships with nitric oxide, RhoA and Rho kinase and oxidative stress systems in GS and BS. In green highlighted the antioxidant and antiremodeling potential. Ang II, angiotensin II; AT1-R, angiotensin II type 1 receptor; [beta] and [gamma] subunit of Gq protein; CO, carbon monoxide; DAG, diacylglycerol; eNOS, endothelial subunit of nitric oxide synthase; ET-1, endothelin-1; G[alpha]q, [alpha] subunit of Gq protein; HO-1, heme oxygenase-1; IP3, inositol triphosphate; MAPK-ERK 1/2, mitogen-activated protein kinases; NE, norepinephrine; PI3K-Akt, phosphatidyl inositol 3-kinase-Akt (protein kinase B); PKC, protein kinase C; PLC[beta], phospholipase C [beta]; P-MLC, phosphorylated myosin light chain; RGS-2, regulatory of the G protein signaling-2; RhoGEF, Rho guanine nucleotide exchange factor; Continuous lines represent stimulation. Dashed lines represent inhibition Adapted from Calò et al. J. Hypertens 32(11):2109-2119, November 2014. (23)

The sodium-chloride cotransporter is a member of the big class of solute carrier proteins (SLC) which include 43 families and 298 transporter genes. [Table 2] In particular, it belongs to the SLC12 of the electroneutral cation-chloride cotransporters and it is encoded by the gene SLC12A3 (36). The SLC12A3 gene transcript variant 1 encodes for human sodium-chloride cotransporter and contains 26 exons with 5582 bp

(NM_000339.2). In situ hybridization experiments showed the presence of the encoding sequence for NCC on the long arm of chromosome 16 region 13 (16q13) (37). SLC12A3 shares a highly conserved aminoacid sequence with other members of the family, which features twelve transmembrane portions harboring a central hydrophobic domain and two cytosolic terminal ends (NH2 and COOH) (38). [Figure5]

The central region seems to be highly specific for ion translocation and for thiazide-binding, particularly the 7th and 8th domains, which entail the external loops fundamental for glycosylation sites (38,39).

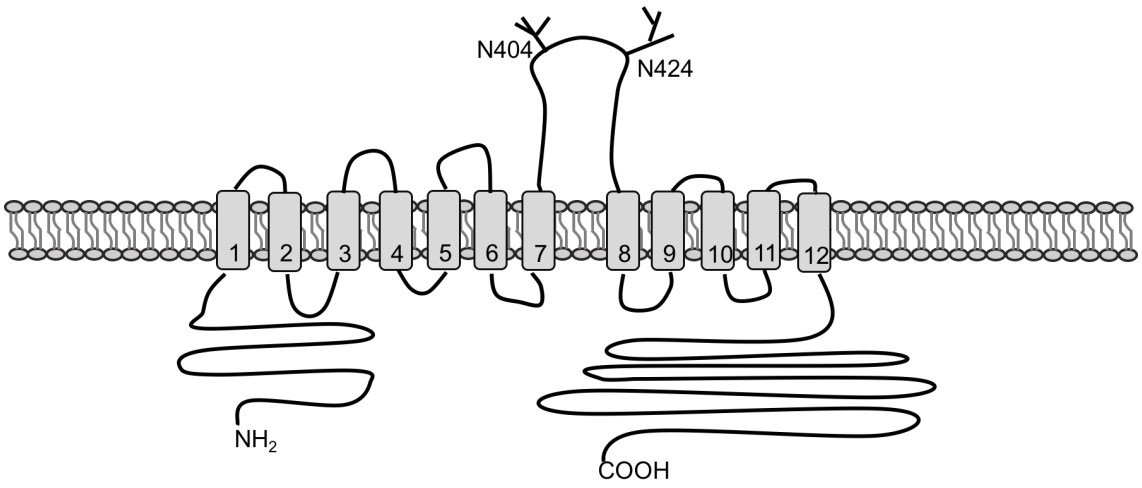

FIGURE 5: Schematic representation of the Na-Cl cotransporter. The N-terminus and C-terminus are in the cytosolic compartment, while the extracellular loop comprised between the 7th and the 8th transmembrane helical traits contains two glycosylation sites (Asparagine 404 and 424).

Symbol	Name	Tot
SLC1	High-affinity glutamate and neutral amino acid transporter family	7
SLC2	Facilitative GLUT transporter family	14
SLC3	Heavy subunits of the heteromeric amino acid transporters	2
SLC4	Bicarbonate transporter family	10
SLC5	Sodium glucose cotransporter family	8
SLC6	Sodium- and chloride-dependent neurotransmitter transporter family	16
SLC7	Cationic amino acid transporter/glyco-protein-associated amino-acid transporter family	14
SLC8	Na^+/Ca^{2+} exchanger family	3
SLC9	Na^+/H^+ exchanger family	8
SLC10	Sodium bile salt cotransport family	6
SLC11	Proton coupled metal ion transporter family	2
SLC12	Electroneutral cation-Cl cotransporter family	9
SLC13	Human Na^+-sulfate/carboxylate cotransporter 5 family	5
SLC14	Urea transporter family	2
SLC15	Proton oligopeptide cotransporter family	4
SLC16	Monocarboxylate transporter family	14
SLC17	Vesicular glutamate transporter family	8
SLC18	Vesicular amine transporter family	3
SLC19	Folate/thiamine transporter family	3
SLC20	Type-III Na^+-phosphate cotransporter family	2
SLC21/ SLCO	Organic anion transporting family	11
SLC22	Organic cation/anion/zwitterion transporter family	18
SLC23	Na+-dependent ascorbic acid transporter family	4
SLC24	$Na^+/(Ca^{2+}$-$K^+)$ exchanger family	5
SLC25	Mitochondrial carrier family	27
SLC26	Multifunctional anion exchanger family	10
SLC27	Fatty acid transport protein family	6
SLC28	Na^+-coupled nucleoside transport family	3
SLC29	Facilitative nucleoside transporter family	4
SLC30	Zinc efflux family	9
SLC31	Copper transporter family	2
SLC32	Vesicular inhibitory amino acid transporter family	1
SLC33	Acetyl-CoA transporter family	1
SLC34	Type-II Na^+-phosphate cotransporter family	3
SLC35	Nucleoside-sugar transporter family	17
SLC36	Proton-coupled amino acid transporter family	4
SLC37	Sugar-phosphate/phosphate exchanger family	4
SLC38	System A and N, sodium-coupled neutral amino acid transporter family	6
SLC39	Metal ion transporter family	14
SLC40	Basolateral iron transporter family	1
SLC41	MgtE-like magnesium transporter family	3
SLC42	Rh ammonium transporter family (pending)	3
SLC43	Na^+-independent, system-L-like amino acid transporter family	2

TABLE 2: List of the Solute Carrier Families

Approximately 400 mutations are described to affect the cotransporter and cause GS. Most of them (~250) are missense [human gene mutation database hgmd.cf.ac.uk] and are spread all along the whole protein. More than 50 mutations have been reported only in Asian populations (38).

Although there are some functional evidences of the impaired activity of NCC mutated, the mechanistic bases of them are still not elucidated yet.

THE ROLE OF NCC IN BLOOD PRESSURE CONTROL

NCC is expressed in the apical membrane of the distal convoluted tubule (DCT) in the kidney where it allows Na^+ and Cl^- reabsorption across the luminal plasma membrane (40-42).

According to an extended structural analysis of the tubules segments, the DCT is the nephron segment that lies immediately downstream of the macula densa and plays a critical role in a variety of homeostatic processes, including sodium chloride reabsorption, potassium secretion, and calcium and magnesium handling. Moreover, it has the capacity to adapt to changes in both hormonal stimuli and the tubular lumen content, thus being fundamental in the control of blood pressure as in the fine tuning of ions excretion (43,44).

Based on expression of the different transporters, DCT can be distinguished in two portions: the early DCT (or DCT1) and the late (or DCT2) (43). NCC is distributed in the DCT1 along with the magnesium channels (TRPM6) and in little part in the DCT2. The DCT2 shows also other proteins, as the target of Aldosterone epithelial sodium channel (ENaC), epithelial calcium channels (TRPV5), the sodium-calcium exchanger (NCX), plasma membrane calcium-ATPase (PMCA), cytoplasmic calcium-binding protein calbindin D_{28k} and intercalated cells (45-48). [Figure 6]

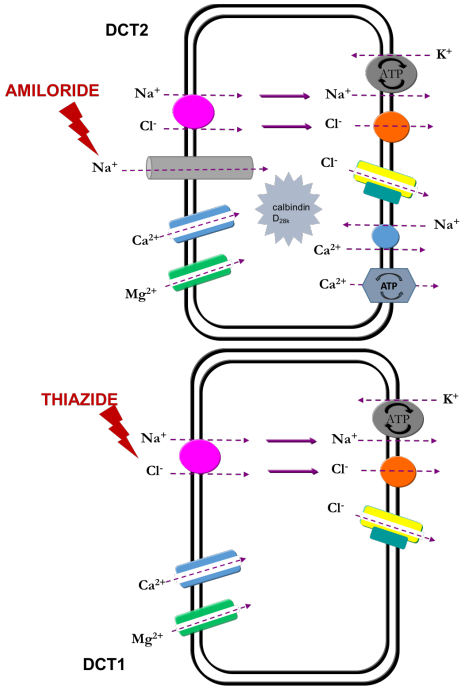

FIGURE 6: schematic representation of DCT1 and DCT2 cells expressing different proteins.

Only 5-10% of the Na^+ load is reabsorbed in the distal convolution and in the connecting tubule (CNT) and micropunture experiments showed that, while the early DCT is sensitive to thiazides, the late DCT is an amiloride-sensitive segment due to the presence of ENaC (49). The Na^+ transport in the DCT1 is electroneutral considering the co-transport of Na^+ and Cl^- trough NCC, while in DCT2 ENaC arise to a negative charge in the tubular lumen for its electrogenic transport of Na^+. The functional significance of a double Na^+ reabsorption is testified by the observation that in low salt experimental condition, ENaC is increased to maintain Na^+ balance (49). As counterpart, to restore a neutral charge in the lumen, potassium secretion is enhanced trough ROMK channels or intercalated cells (43). The interplay between Na^+ reabsorption and K^+ secretion is fundamental to understand pathological conditions, in which there is a gain-of-function or a loss-of-function of certain proteins. NCC loss-of-function mutations lead to Na^+ dissipation, which in turns stimulate a gradient for water to exit, whereas ENaC overactivates to restore the Na^+ intake. Finally, to replace the ionic imbalance in the tubular lumen, ROMK drives K^+ out leading to hypokalemia. On the contrary, in gain-of-function conditions, overstimulation of NCC prompt to hypertension and hyperkalemia can be observed in patients with pseudohyperaldosteronism type II (Gordon's syndrome) (50).

Cotransporters and channels coordination is the driving force that permit the fine tuning of ions in the DCT. Magnesium absorption through TRPM6 is potentiated by apical K channel Kv1.1 which generates the lumen negative potential. Basolateral K channel Kir4.1 and the of Na,K-ATPase also increase magnesium reabsorption by creating a sodium gradient, enabling NCC to transport sodium from the apical lumen to the cytosol (Blaine).

As the over-activation of RAAS is a feature of Gitelman's syndrome, the presence of high plasma aldosterone levels burden on the DCT, but the effect may differs along the axis of the distal convolution (42). Studies in rat demonstrated that MR is present in the DCT and in the CNT, albeit the enzyme 11β-hydroxysteroid dehydrogenase type 2 (11β-HSD2 which in turns, inactivates glucocorticoids that would otherwise occupy aldosterone receptors), seems to be detectable only in the late DCT (50,51).

Studies in rat showed that whereas MR seems to be present throughout the DCT and CNT, 11β-HSD2 is not detectable in the early DCT1 but is well detectable in the late DCT (DCT2), in the CNT, and CD(47,52). These investigations suggest that aldosterone may stimulate sodium-transport mainly in the DCT2 where ENaC, NCC,

MR and 11β-HSD2 are expressed, while in the early DCT, NCC activity could be stimulated by mineralcorticoids and glucocorticoids in combination (53).

FUNCTIONAL STUDIES

Transfection experiments can be regarded as a powerful strategy to understand gene function and have been widely used to highlight many biological issues. By transfection technique is possible to introduce exogenous genetic information in a host cell in order to induce the production of certain protein and more generally to study biochemical pathways. The methods in which the DNAs or RNAs are delivered varies according to the purpose and the host chosen. Ideally, procedures should have high transfection efficiency, low cell toxicity, minimal effects on normal physiology, and be easy to use and reproduced (54).

Three typical transfection methods exists: the biological, the chemical and the physical, each of them presenting advantages and disadvantages. Biological methods are performed by inserting viral vectors in the host. The viral DNA integrates randomly in the host genome and permits a high efficiency in terms of transfection, nevertheless, during the process some mutations not predicted can arise, leading therefore to a final abnormal cell (55). Chemical methods are the most commonly used for their easiness of procedure and no contamination of genetic information, but still the efficiency can vary for a considerable number of factors. The ratio between chemicals and DNA, the cells growth rate, pH of the solutions and the timing of the experiments influence the response. Among chemical transfections can be considered cationic polymer (one of the oldest chemicals used), calcium phosphate, cationic lipid (the most popular method), and cationic amino acid (56). Micro injection, biolistic particle delivery, electroporation, and laser-based transfection are physical procedures to deliver exogenous DNA but can be expensive and need a arrangement of the protocols (57).

➢ *HUMAN EMBRYONIC KIDNEY CELL LINE*

HEK293 is a cell line derived from human embryonic kidney cells grown in tissue culture. They have been originally transfected with the calcium phosphate medium exposure for 3 days and later on with low calcium ion medium, to and Adenovirus type 5 purified DNA (Ad_5 DNA) of approximately 4.5 kilobases. After the viral transfection, the HEK293 cell line showed significantly disrupted cell morphology with a tendency to growth in clumps and to replicate fast (58).

One of the most well established method of transfection is lipofection. [Figure 7]. The underlying principle is that positively charged chemicals complexes with negatively charged nucleic acids. These positively charged complexes are attracted to the negatively charged cell membrane. To date, no experimental evidences clarified how the complexes pass through the cell membrane; however, supposedly this occurs via endocytosis.

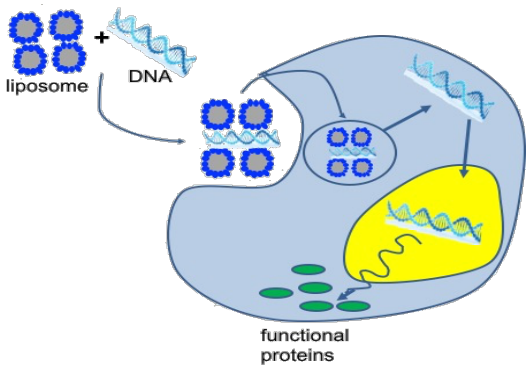

FIGURE 7: Schematic process of lipofection. The negative charged DNA binds the positively charged liposomes. The complex is thus attracted by the cell membrane. Once in the cytosolic compartment, the complex releases the DNA which in turns enters into the nucleus of the host and codify for the specific information introduced.

➢ *XENOPUS LAEVIS OOCYTES IN BIOLOGY*

Xenopus is a genus of African frogs that are commonly known as the African clawed frogs. Originally frogs were used as a test for pregnancy by revealing the presence of chorionic gonadotropin released in women urines (59). After stimulation by the hormone, frogs produce a huge number, often thousands, of eggs (also defined oocytes) and this indicated the presence of gestation. X.L. oocytes are therefore, a useful tool for biochemical investigation, especially of membrane transporters and channels (60). The oocytes have a diameter of 1.2 mm which permits to manipulate them easily. During the first stages of development they are rich in RNA and proteins and they lack of a transcriptional activity until the mid-late blastula stage. Visually they appear divided in two hemispheres, the vegetal pole and the animal one. The vegetal pole is white colored and is characterized by the presence of yolk cells organized in a blastula with slow division. The animal pole, the darker and opaque hemisphere, consists of small cells that divide rapidly (61).

The elevated number of eggs produced can be easily conserved in a saline solution and manipulated by injecting exogenous material as DNA codifying for one or more proteins of interest (59). The step by which the procedure undergoes start from a sorting of the "visually healthier" eggs from the batch, followed by a defolliculation phase by either enzymatic or manual treatment (62). [Figure 8]

FIGURE 8: Process of defolliculation of Xenopus Laevis oocytes. The dark and the white hemispheres indicate the animal pole and the pole respectively.

After the defolliculation step, which removes the follicle layer anchored to the vitelline one, RNA can be injected. X.L. oocytes are being successfully used to investigate ions channels and cotransporters activity, because of their low level of endogenously expressed channels and receptors, which yields a relatively electrophysiologically silent background. Moreover, they also carry the cellular apparatus to produce functionally post-translational modifications (63).

AIM OF THE STUDY

This study aims to characterize the molecular and functional effects of a novel point mutation (c.1204G>A) that was found in a GS case, never described before. The mutation causes the aminoacid exchange Gly394Asp in the 7th transmembrane domain of the cotransporter, which is an important site close to the two glycosylation residues of the protein. In order to assess the impact of this exchange on the activity of the protein, the study has been conducted following the study design:

MATHERIALS AND METHODS

Investigation strategy

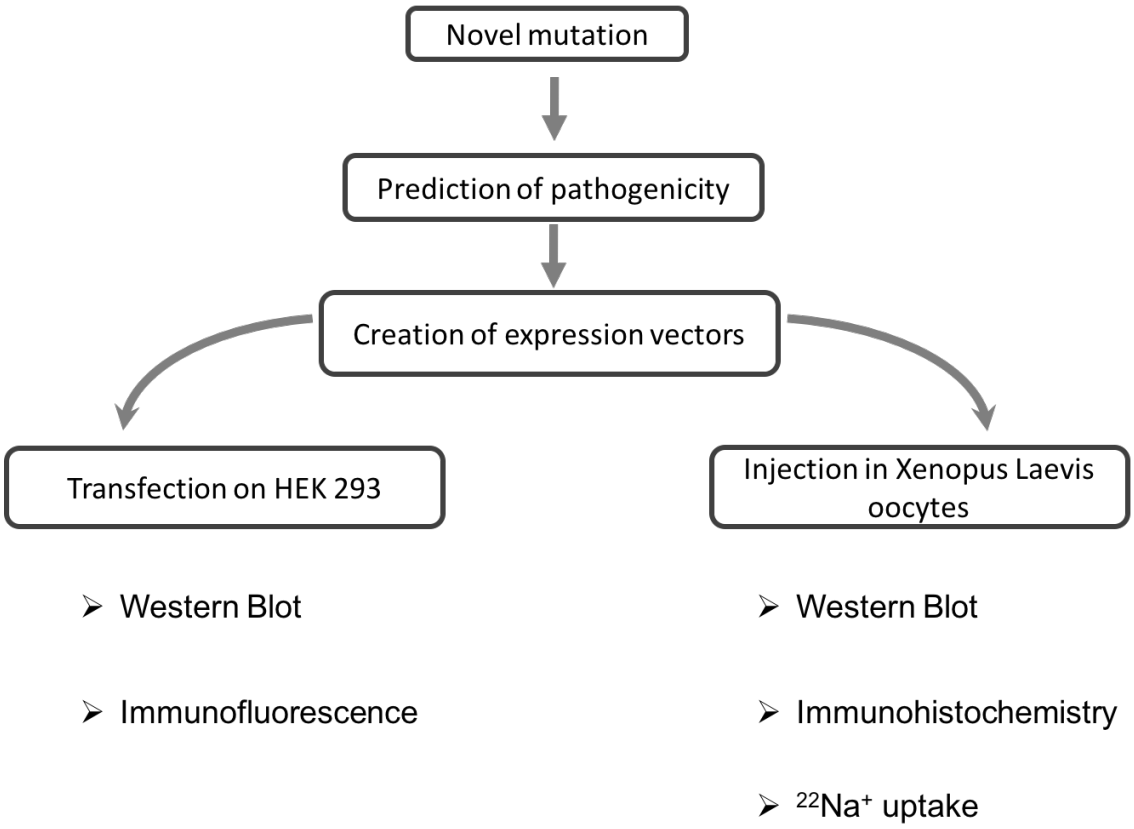

After the genetic screening the patient has been afterwards diagnosed for GS. In order to predict the possible impact of the novel mutation in the activity of the cotransporter has been conducted a research by using bioinformatics tools. Taking into account all the results, construct expression vectors enclosing the genetic information for either NCC wild-type and NCC mutated (G394D-NCC) have been created. After optimization of the protocols, constructs have been transfected in HEK293 cells in which the grade of protein expression has been evaluated by immunofluorescence and western blot. Beside the in vitro experiments, oocytes coming from Xenopus Laevis frog have been injected with the constructs and have been used for immunohistochemistry analysis, western blot and for $^{22}Na^{+}$ uptake experiments.

Molecular Investigation

After a clinical diagnosis of Gitelman's syndrome, was made a genetic test was done to confirm the diagnosis and identify possible mutations on the SLC12A3 gene. This was done at the Laboratory of Medical Genetics (Ospedale Maggiore Policlinico, Fondazione IRCCS Ca' Granda, Milano), certified by the European Molecular Genetics Quality Networ (www.emqn.org)

DNA was extracted from a peripheral blood sample and all 26 exons were analyzed.

Prediction of mutation influence

Phenotypic effects of amino acid substitution on protein function were predicted by online bioinformatics tools. At least two of them should give an indication of potential impairment.

I-Mutant2.0, (http://folding.biofold.org/i-mutant/i-mutant2.0.html) to predict the stability; Polyphen-2 (http://genetics.bwh.harvard.edu/pph2/) to predict the pathogenicity and Sorting intolerant from tolerant SIFT (http://sift.jcvi.org) to predict the activity of the protein mutated) (64-66). To confirm the results of SIFT, an additional tool was used: the Protein Variation Effect Analyzer (PROVEAN, http://provean.jcvi.org/index.php). The latter, accepts a protein sequence and amino acid variations as input, performing a BLAST search to identify homologous sequences (supporting sequences), and generating PROVEAN and SIFT scores.

Synthesis of wt-NCC and G394D-NCC cRNA

cDNA (GeneCopoeia, Rockville, USA) of human wild-type (wt-NCC) and mutated NCC (G394D-NCC) were cloned in pSDeasy vector. After linearization of the plasmid with PciI (New England Biolabs) cRNA synthesis was performed using the MEGAScript SP6 kit (ambion; USA) following the manufactures instructions. cRNA was purified (Nucleospin RNA; MacheryNagel, CH) and the integrity of the transcription product was confirmed by agarose gel electrophoresis.

cRNA injection in X. laevis Oocytes

X. laevis oocytes of stage IV-V were injected with 0.05µl cRNA (44µg/µl) of wt-NCC and G3964D-NCC respectively or, as a control, with 0.05µl H_2O. Oocytes were incubated at 16°C for 72 h in modified Barth's Solution (NaCl 88mM, KCl 1mM, $CaCl_2$ 0.41mM, $MgCl_2$ 0.82mM, $Ca(NO_3)_2$ 0.33mM, $NaHCO_3$ 2.4 mM, HEPES/Tris 10 mM, pH 7.4) with gentamycin (5mg/l) and Doxy for translation of the protein. Solutions were changed daily. After 72 h oocytes were processed to analyze NCC expression, trafficking and activity by western blot, immunohistochemistry and $^{22}Na^{+}$-uptake experiments respectively.

Western blot

For Western blot experiments, 3 to 10 oocytes per group were pooled and lysed in 30 to 100 µl lysis buffer (10µl lysis buffer/oocyte; 250mM Sucrose; 0.5 mM EDTA, pH8; 5 mM Tris-HCl, pH 6.9; Protease Inhibitor (Roche Diagnostic; Mannheim, D) and Phosphatase Inhibitor (Roche Diagnostic; Mannheim, D)). Proteins (an equivalent of one oocyte per lane) were separated in a SDS-PAGE gel and transferred on nitrocellulose membrane. Membrane was blocked by odyssey blocking buffer and NCC was detected with an antibody against the N-terminal tail of NCC (1:4000; Millipore) followed by a goat anti rabbit IRD800 (1:20'000; LI-COR, Bad Homburg, Germany) and subsequent imaging with the LI-COR system (LI-COR, Bad Homburg, Germany). Equal protein loading was controlled by immunodetection of GAPDH with a mouse monoclonal antibody (1:4000; Ambion, Carlsbad USA)

Immunofluorescence

For immunofluorescent studies, oocytes were fixed with 3%PFA in 0.1M phosphate buffer (pH7.3; 300 mosm) for 4 hours at 4°C and rinsed in phosphate buffer for an additional 2 hours. Afterwards, oocytes were frozen in liquid propane, stored at -80°C, and then processed for immunofluorescence similar to previously described procedures (67). In brief, frozen oocytes were cut in a cryostat in 5 µm thick sections. Unspecific binding sites were blocked with 10% normal goat serum and 1% bovine serum albumin in PBS. Cryosections were incubated overnight at 4°C with an antibody against the N-terminal tail of NCC (1:2000; Millipore). Binding sites of the first antibody were detected using a CY3 labelled goat-anti-rabbit antibody (1:1000;

Jackson Immuno Research, West Grove, PA, USA. The cell surface of the oocytes was labeled by detecting the microvillar actin cytoskeleton with Fluorescein Phalloidine (1:50; Biotium, Hayward, USA). After repeated washings, sections were cover slipped and studied with a fluorescence microscope (Leica DM6000 B). Images were acquired with a CCD camera and processed by Adobe Photoshop and Microsoft Power Point software.

$^{22}Na^{+}$-uptake experiments

For $^{22}Na^{+}$ uptake experiments was followed the protocol from Monroy et. al. (2001) (68). 72h after infection, oocytes were washed and incubated for 30 minutes at 30°C in isotonic K^{+}- and Cl^{-}-free medium (Na^{+}-gluconate, 96mM; Ca^{2+}-gluconate, 6mM; Mg^{2+}-gluconate, 1mM; HEPES/Tris (pH 7.4), 5mM; ouabain, 1mM, bumetanide, 100 µM; amiloride 100 µM). Uptake was performed at 30°C for 60 minutes in an isotonic K^{+}-free medium (NaCl, 96mM; $CaCl_2$, 1.8mM; Mg Cl_2, 1mM; HEPES (pH 7.4), 5mM; ouabain, 1mM, bumetanide, 100 µM; amiloride 100 µM) supplemented with 2 µCi/ml $^{22}Na^{+}$ (Perking Elmer, Waltham, MA, USA). To determine thiazide dependent sodium-uptake, uptake was performed in presence or absence of a thiazide-like diuretic (100µM Metolazone in DMSO; Sigma-Aldrich). $^{22}Na^{+}$ uptake was terminated by washing the oocytes 6 times in ice-cold K^{+}-free medium to remove extracellular $^{22}Na^{+}$. Oocytes were individually lysed in 10% SDS. Radioactive tracer was detected in a liquid scintillation analyzer (Packard TRI-CARB 2000/2200CA; PerkinElmer, USA).

Results of three individual experiments were pooled (wt-NCC (Nno Thiazide=44; NThiazide=46), G394D-NCC (Nno Thiazide=44; NThiazide=42), H2O (Nno Thiazide=43; NThiazide=44)).

In vitro experiments

The human embryonic kidney cell line HEK-293 (American Type Cell Culture, ATCC, Manassas, VA), which was originally transformed by exposing cells to sheared fragments of adenovirus type 5 DNA (58), was used as a model of kidney cells for the ease of growth and transfection efficiency. Cells were cultured in Eagle's Minimum Essential Medium added with 10% fetal bovine serum (FBS) (Sigma Aldrich) in Corning® T-75 flasks at 37°C and 5% CO_2. After replication of expression vectors ORF cDNA clones (GeneCopoeia, Maryland, USA) by bacteria, wt-NCC, G394D-NCC

and green fluorescent protein (GFP) DNAs were transfected into the cells by lipofection technique using Metafectene® (Biontex Laboratories GmbH, München, D). Lipofection technique was chosen for its high efficiency, low toxicity and high reproducibility established in our laboratory. After protocol optimization cells were stimulated cells at 24 and 48 hours of transfection.

Immunoblotting

To evaluate NCC protein expression proteins were extracted from the cells transfected by using a lysis buffer (150mM NaCl, 50mM Tris-HCl pH 8.00, 1% Triton-X-100, Protease and Phosphatase Inhibitors, Roche, BS, Switzerland). To quantify proteins, a Bradford assay with standard protocol was performed (CooAssay Protein Dosage Reagent, Uptima, France). Protein samples were separated in an 8% polyacrylamide gel. After electrophoretic separation, proteins were transferred to nitrocellulose membranes which were then blocked for 30 minutes in blocking buffer (Odyssey blocking buffer, Li-Cor Biosciences, USA) and incubated with primary antibodies against NCC (Millipore) diluted 1:4000 at 4°C overnight. Membranes were further incubated for 2 h with goat anti rabbit IRD800 (1:20'000; LI-COR, Bad Homburg, Germany) diluted 1:10000 and finally visualized by Odissey imager (Li-Cor, Nebraska, USA). A monoclonal antibody against α-tubulin diluted 1:10000 was used for normalization. Images were processed and analyzed using a densitometric semiquantitative analysis with NIH image analyzer software (NIH ImageJ; Fiji open-source).

Immunofluorescence

To detect whether the cells acquired the plasmids, cells were let growing on glass coverslips and after transfection with wt-NCC, G394D-NCC and GFP DNAs, were fixed at 4°C with the fixation solution (PFA 3%, PBS pH 7.3). After over night fixation and 3 times washing steps with PBS, cells were pre-incubated with PBS/BSA2% 10 minutes, followed by incubation with 0. 5% Triton-100 and washing steps, finally incubated with an anti-N-terminal tail of NCC antibody diluted 1:2000 over night at 4°C. The following day coverslips were rinsed and incubated 2 h at dark with a secondary CY3 labelled goat-anti-rabbit antibody diluted 1:1000 (Jackson Immuno Research, West Grove, PA, USA), and DAPI diluted 1:1000 and PBS/BSA2%

for nuclei staining and after washing steps, the glycerol mounting medium with DABCO was added and left 2h at 4°C. Images were revealed with a confocal Leica microscope. Images were acquired with a CCD camera and processed by Adobe Photoshop and Microsoft Power Point software.

Power calculation and statistical analysis

Sample size were preliminarily calculated by ImageJ software, then analyzed with GraphPad Prism 5. A two-way analysis of variance (ANOVA) was used to assess both the differences between wt-NCC and G394D-NCC glycosylation and the $^{22}Na^{+}$ Uptake in the oocytes experiments.

RESULTS

Prediction of mutation influence

The novel mutation found in the index case, is a single nucleotide c.1204G>A (ref. NM_000339.2), which induces the exchange of a Glycine with an Aspartic Acid in position 394. The meaning of the mutation can be predicted by using software that forecast the possible impact of an amino acid substitution on the structure and function of a human protein matching with bioinformatics tools the physical and comparative considerations. I-Mutant2.0, Polyphen-2 and SIFT are three online programs useful to predict the stability, pathogenicity and the activity respectively of a mutation (http://folding.biofold.org/i-mutant/i-mutant2.0.html, http://genetics.bwh.harvard.edu/pph2/, http://sift.jcvi.org). The relevance of these tools, even if there might be some inaccuracy in the results, occurs when it is necessary to screen many variants to characterize them. When the linear amino acids sequence is translated into a three dimensional protein structure, it delineates alpha-helices and β-sheets strands, which tends to arrange in a specific thermodynamically most stable conformation (69). If there is some perturbation of the system, the protein can not be folded in the proper shape leading to production of an erroneous peptide. The cell machinery deputed to dismantle it is therefore activated. Alignment of the human sequence with other orthologous species, reveals a high degree of conservation, especially for the region between the 7^{th} and the 8^{th} transmembrane portions among them (37).

- *Prediction of NCC mut activity with SIFT and PROVEAN programs:*

SIFT prediction is based on the degree of conservation of amino acid residues in sequence alignments derived from closely related sequences. Those with SIFT score ≤0.05 were classified as deleterious and those >0.05 were classified as tolerated (doi: 10.1038/nprot.2009.86). The mutation in 394 of a Glycine (G) with an Aspartic Acid (D) has a SIFT score ≤0.05 thus is classified as not tolerated in a highly conserved region. [Figure 9]

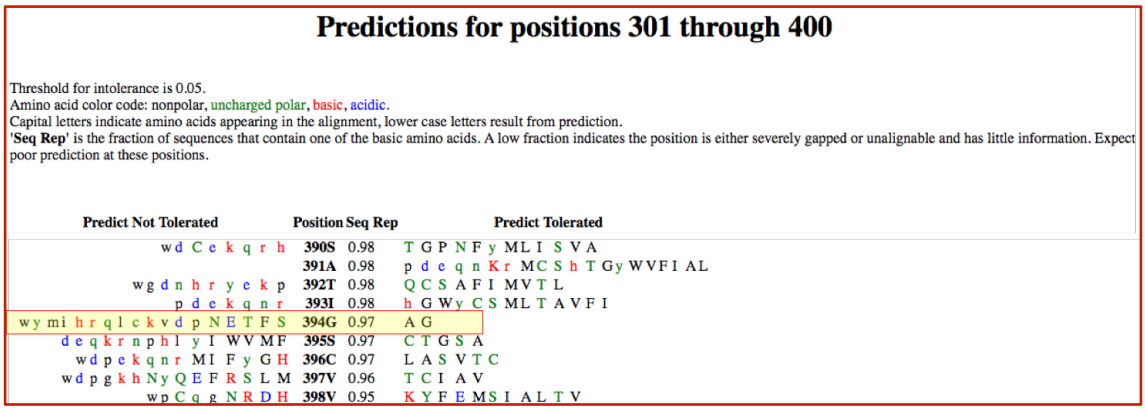

Predictions for positions 301 through 400

Threshold for intolerance is 0.05.
Amino acid color code: nonpolar, uncharged polar, basic, acidic.
Capital letters indicate amino acids appearing in the alignment, lower case letters result from prediction.
'Seq Rep' is the fraction of sequences that contain one of the basic amino acids. A low fraction indicates the position is either severely gapped or unalignable and has little information. Expect poor prediction at these positions.

Predict Not Tolerated	Position	Seq Rep	Predict Tolerated
w d C e k q r h	**390S**	0.98	T G P N F y M L I S V A
	391A	0.98	p d e q n K r M C S h T G y W V F I A L
w g d n h r y e k p	**392T**	0.98	Q C S A F I M V T L
p d e k q n r	**393I**	0.98	h G W y C S M L T A V F I
w y m i h r q l c k v d p N E T F S	**394G**	0.97	A G
d e q k r n p h l y I W V M F	**395S**	0.97	C T G S A
w d p e k q n r M I F y G H	**396C**	0.97	L A S V T C
w d p g k h N y Q E F R S L M	**397V**	0.96	T C I A V
w p C q g N R D H	**398V**	0.95	K Y F E M S I A L T V

FIGURE 9: the yellow row highlights the position of the aminoacid exchange. The d in blue is the aspartic acid in the right lane, which means that is not accepted as exchange, because if would influence in the activity of the protein.

To confirm the result, a PROVEAN job was also submitted using the following input format: <protein ID> <position> <reference aa> <variant aa>

The score of -5.71 (reference value = -2.5) predict a deleterious phenotype, and confirmed the SIFT score below the threshold of ≤0.05. [Figure 10]:

VARIATION		PROTEIN SEQUENCE CHANGE			
ROW_NO.	INPUT	PROTEIN_ID	POSITION	RESIDUE_REF	RESIDUE_ALT
1	NP_000330.2 394 G D gitelman .	NP_000330.2	394	G	D

PROVEAN PREDICTION				SIFT PREDICTION			
SCORE	PREDICTION (cutoff=-2.5)	#SEQ	#CLUSTER	SCORE	PREDICTION (cutoff=0.05)	MEDIAN_INFO	#SEQ
-5.71	Deleterious	256	30	0.000	Damaging	2.88	254

Figure 10: PROVEAN score for the prediction of the impact of a mutation on biological function of the protein.

➢ *Prediction of NCC mut stability with I-Mutant2.0*

I-Mutant software predicts that the mutation destabilizes the free-energy energy leading to a protein structure not fixed. [Figure 11]

Position	WT	NEW	Stability	RI	pH	T
394	G	D	Decrease	9	7.0	25

Figure 11: The software gives the prediction of decreased stability based on a high reliability index (9) at a temperature of 25 °C and pH 7.0. (**WT**) aminoacid in Wild-Type Protein, (**NEW**) New Aminoacid after Mutation, (**RI**) reliability Index, (**T**) temperature in Celsius degrees, (**pH**) $-\log[H^+]$

➢ *Prediction of NCC mut pathogenicity with PolyPhen-2*

PolyPhen-2 gave a high score, indicating a possible impact as damaging. [Figure 12]

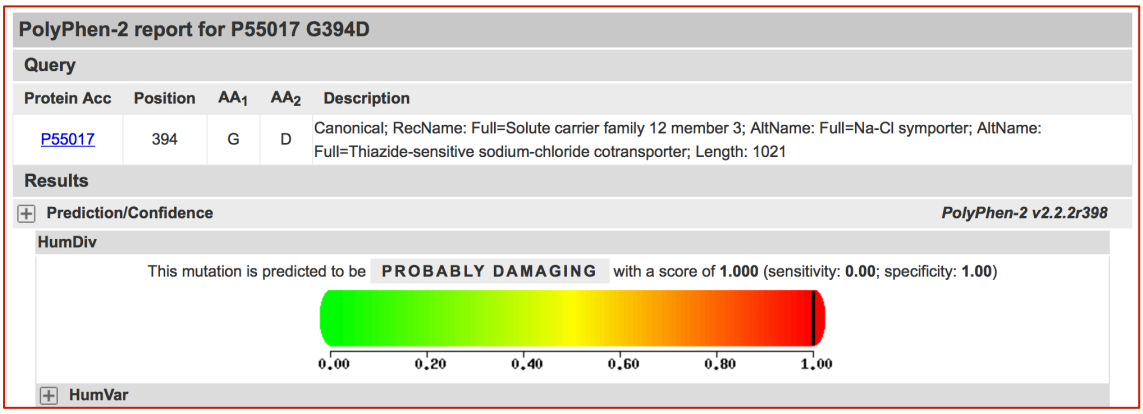

Figure 12: Image of PolyPhen-2 analysis for the Gly394Asp. The high score of 1.00 indicate the amino acid exchange probably damaging.

HEK293 Transfection

Cells were transfected by using liposome technique with three exogenous DNAs containing the information of the while type protein, of the mutant respectively and the information for the green fluorescent protein (GFP). Plasmids were produced introducing the mutation found in the index case: the nucleotide exchange in position 1204 of a guanine with an adenine produced therefore an Aspartic Acid in spite of the Glycine in position 394. The folding structure of the cotransporter reveals the mutation to be sited near the extracellular loop containing the two glycosylation sites of the aa in 404 and 424 [Figure 13].

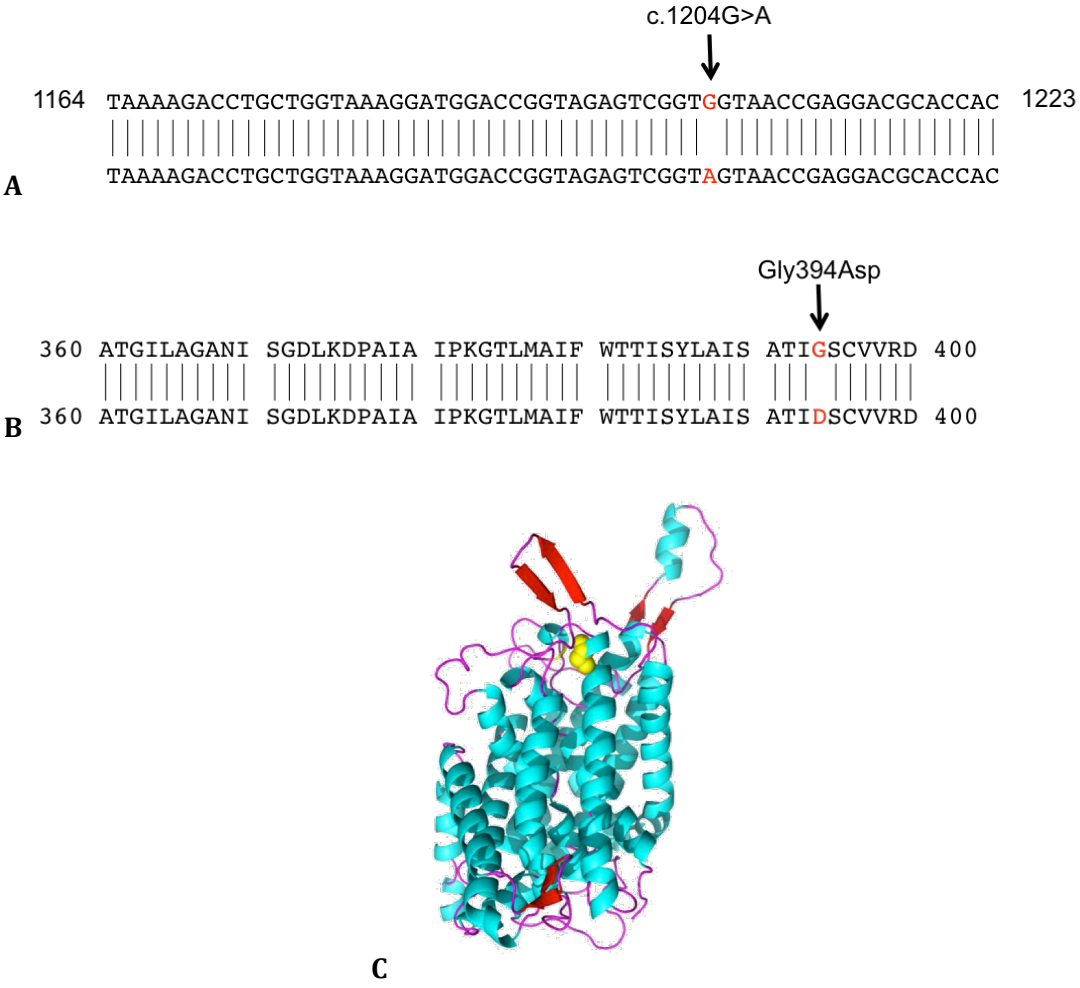

FIGURE 13: A. Alignment of the wild-type and the mutant nucleotide sequences. **B**. Alignment of the wild-type and the mutant amino acid sequences. **C**. Three-dimensional image of the sodium-chloride cotransporter NCC. Highlighted in yellow is the point mutation in the seventh transmembrane portion, near the extracellular loop.

Transfection efficiency was assessed by immunofluorescence in Hek293 cell line using cells transfected with genetic information for the green fluorescent protein as control. We observed the rate of growth of the cells and, by according to protocol, transfected when they were at 70% of visual confluence. GFP transfected cells were green under fluorescence microscope, while those transfected with G394D-NCC or wt-NCC were not. This result indicates that there was no error in the replication and isolation of the plasmids. Moreover, to assess if the genetic information was correctly transmitted to the host, immunostaining using an antibody for NCC was performed. The GFP cells did not show any staining for NCC antibody when assessed at the confocal microscope, as proof of good quality transfection [Figure 14].

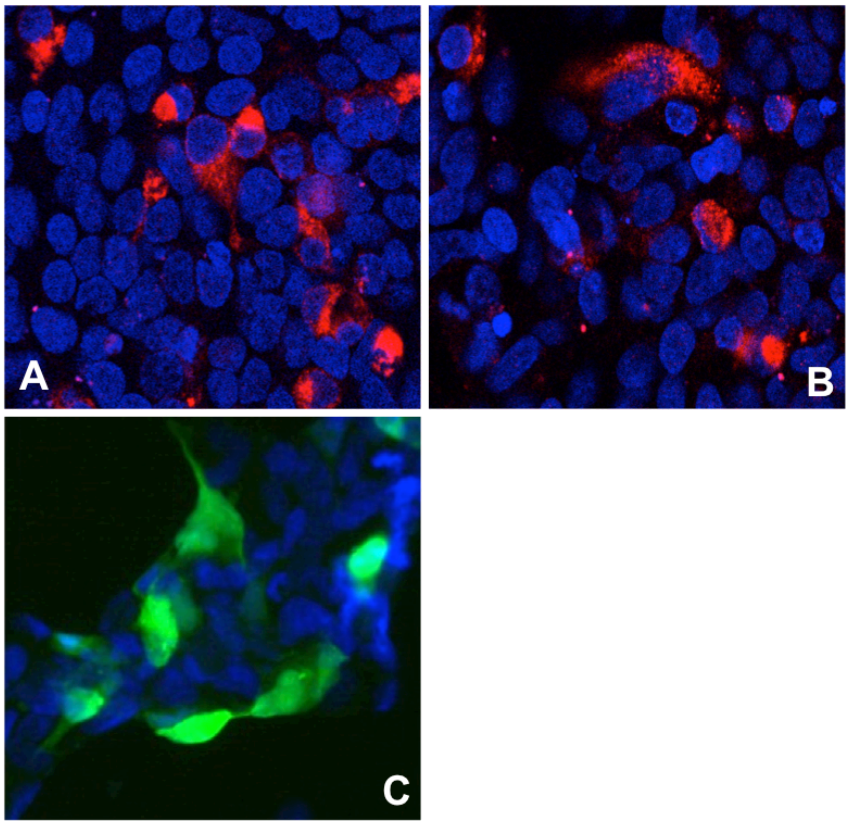

FIGURE 14: Immunofluorescence on HEK293 with 20X zoom. **A**: Cells transfected with wt-NCC. **B**: Cells transfected with G394D-NCC. **C**: Cells transfected with EGFP. In blue DAPI staining, in red staining for NCC. Cells transfected with EGFP do not show staining for NCC.

- *NCC Glycosylation in HEK293 cells line*

To investigate whether if the novel mutation affects protein glycosylation, both the samples treated with wt-NCC and with G394D-NCC were blotted and a difference in the proteins glycosylation was observed. Wt-NCC showed a higher band (around 130KDa), while the mutant did not. When the two bands were quantified, we found a significant difference of the higher band expression at 24 hours ($p<0.003$ NCC wt mean + SEM 0,233±0.046; NCC mut mean + SEM 0.0268±0.008) in the wild type compared to the mutants and an even more prominent difference was at 48 hours of transfection ($p<0.0003$ wt-NCC 0,524±0.084; G394D-NCC 0.059±0.012). [Figure 15]

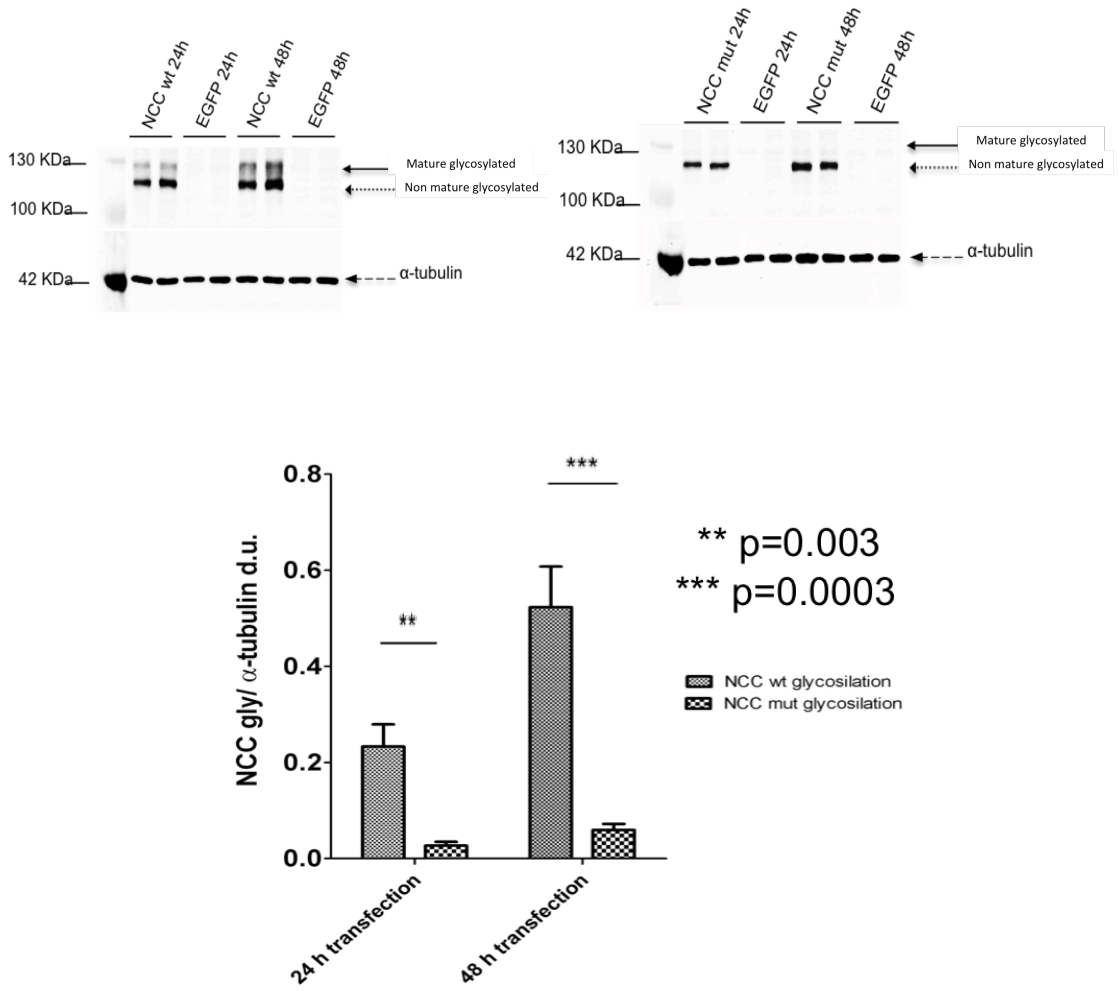

FIGURE 15: A Immunoblots representative of cells transfected with wt-NCC gene and G394D-NCC gene. Full and dotted arrows point out the mature glycosylated and the non-mature glycosylated band respectively. α-tubulin was used as housekeeping gene. **B** Mature glycosylated protein expression calculated in density units normalized for α-tubulin after 24 and 48 hours of transfection

Xenopus laevis oocytes experiments

Expression vectors were created by ligation of the psDeasy BS backbone with an insert of hNCC wt, G394D-NCC and EGFP. A first experiment was performed to assess the efficiency of the injection, by using only the EGFP construct. Oocytes, after 24 hours of injection expressed the green fluorescent proteins visualized at the florescent microscope. [Figure 16]

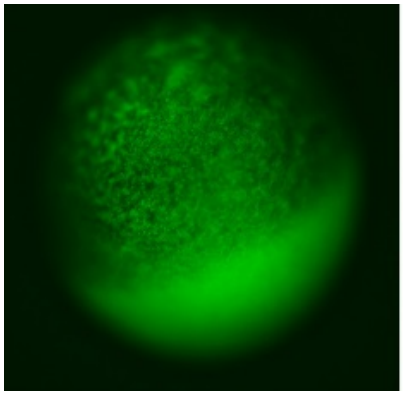

FIGURE 16: X.L. oocyte expressing green fluorescent protein. The animal pole is in the upper hemisphere, while the vegetal pole is the white hemisphere.

- *X.L. oocytes western blot*

The X.L. oocytes lysate was used to western blot experiments for the detection of the NCC protein expression. Wild-type NCC injected oocytes showed after 24 hours and after 48 hours a band around 130KDa while G394D-NCC did not. The band was even more predominant at 48hours of injection. [Figure 17]

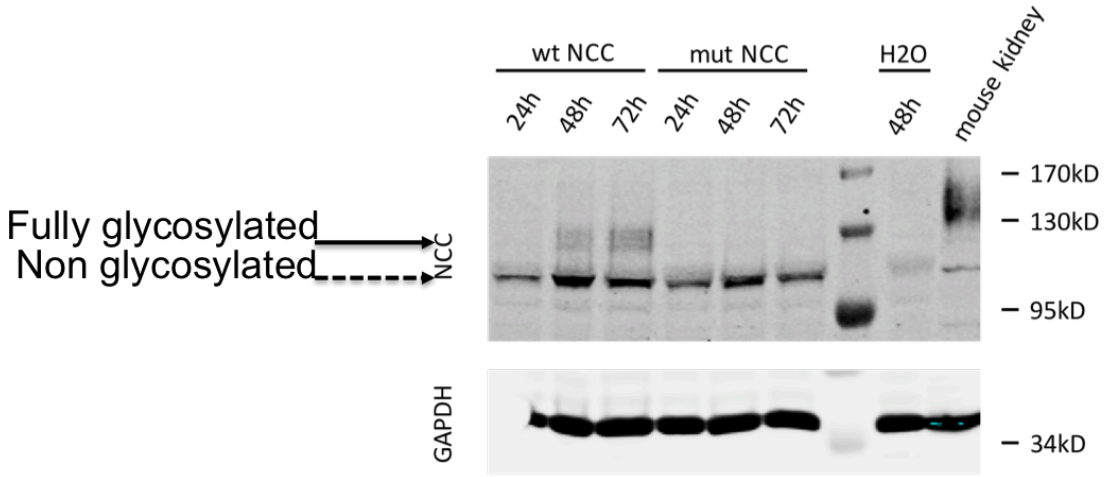

FIGURE 17: western blot image of oocytes lysate blotted with an antibody against NCC. Around 130KDa wt NCC expresses a higher band of fully glycosylated protein, while mutant does not. Antibody against GADPDH was used as loading control.

➢ *X.L. oocytes immunohistochemistry*

In X.L. oocytes injected with either human NCC wild-type RNA or mutated (c.1204G>A) RNA, immunohistochemistry experiments showed a difference between the phenotypes. Using antibodies against NCC, in oocytes expressing wt-NCC a staining for the protein was observed at the membrane surface of the oocytes. By contrast, in those injected with G394D-NCC RNA, antibody against NCC was detectable under the membrane surface. The cell surface of the oocytes was labeled by detecting the microvillar actin cytoskeleton with Fluorescein Phalloidine as housekeeping marker. Merged images showed an overlay between actin and NCC in wt-NCC expressing oocytes. No overlay of G394D-NCC oocytes with actin staining was found. [Figure 18]

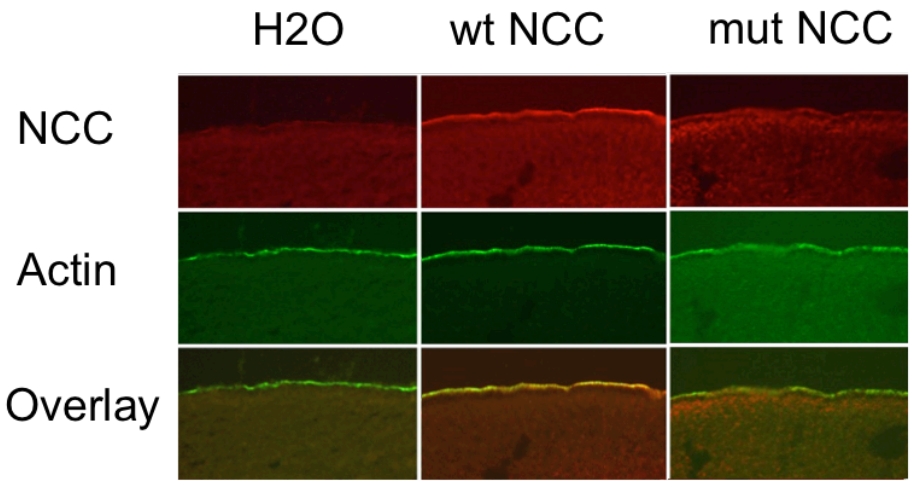

FIGURE 18: Immunohistochemistry analyses of oocytes injected with 0.05µl H_2O as vehicle, wt-NCC, G394D-NCC cRNA respectively. Co-labelling with both the antibodies for NCC and actin. Actin cytoskeleton is used as housekeeping marker and shows the staining at the membrane. wt-NCC stains at the membrane as the overlay with actin is clear, while G394D-NCC stains under the membrane.

- *X.L. oocytes $^{22}Na^{+}$ uptake*

Functional studies were performed by using $^{22}Na^{+}$ uptake to confirm the phenotypes. Three independent experiments were done in different conditions: controls were oocytes injected with water, mutated were oocytes injected with G394D-NCC, and wild-type were injected with wt-NCC. Each group was either treated or not with thiazides.

In physiological conditions, controls group absorbed a low quantity of $^{22}Na^{+}$ set as 100% and when challenged with thiazide treatment showed less, but not significant, uptake (without thiazide 100 vs. with thiazide 65.01 $p>0.05$). wt-NCC oocytes could absorb $^{22}Na^{+}$ more than 3 folds compared to controls (342.3), meaning that the insertion of the protein was effective in terms of reaching the membranes and explicating its activity. When thiazides were added to wt-NCC, the cotransporter activity was significantly inhibited resulting in a drop of uptake (without thiazide 342.3 vs. with thiazide 63.3 $p<0.0001$). By contrast, G394D-NCC resulted in no $^{22}Na^{+}$ uptake in both conditions, regardless of the presence or absence of thiazides (without thiazide 77.3 vs. with thiazide 75 $p>0.05$) [Figure 19].

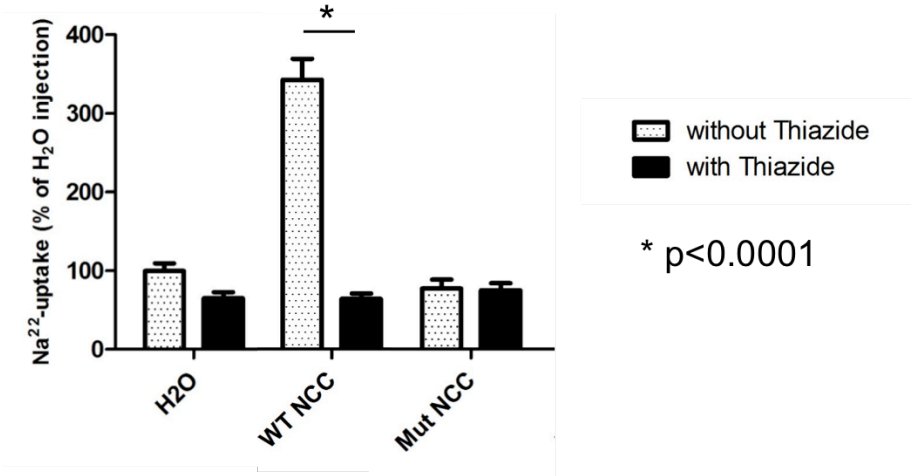

FIGURE 19: $^{22}Na^{+}$ Uptake in oocytes injected and treated or not treated with thiazides. Control group H_20: without thiazide 100 vs. with thiazide 65.01 $p>0.05$; WT NCC: without thiazide 342.3 vs. with thiazide 63.3 $p<0.0001$; Mut NCC (G394D-NCC): without thiazide 77.3 vs. with thiazide 75 $p>0.05$

This result confirms the relevance of NCC function for Gitelman phenotype: the point mutation characterized leads to lack of intrinsic activity of the protein resembling the impaired $^{22}Na^{+}$ uptake induced by thiazide treatment.

DISCUSSION AND CONCLUSIONS

This study aimed at characterizing a novel mutation found in the sodium chloride cotransporter in a heterozygous patient affected by Gitelman's syndrome. NCC is a member of the solute carrier family 12 (SLC12) of electroneutral cation coupled cotransporter family (70-72). This cotransporter shares a highly conserved aminoacid sequence with other members of the family. It features twelve transmembrane portions harboring a central hydrophobic domain and two cytosolic terminal ends (NH_2 and COOH) (38).

Standing from the clinical identification of a patient with a complete biochemical characterization pointing to a diagnosis of GS, we performed a genetic analysis for the 26 exons of SLC12A3 gene. This led to identify two mutations: c.1925G>A (Arg642His) and c.1181G>A (Gly394Asp). The former is one of the most common variant described in the syndrome, but the latter has never been described before. Since not all the variants are causative of the pathology, this prompted us to investigate which was the relevance of the novel mutation (Gly394Asp) for the phenotype and the clinical outcome.

By using bioinformatics tools for the prediction of the mutation impact in the protein activity, the novel mutation seems to have a stronger impact compared to the other present, in fact the PROVEAN score was -5.71 for G394D vs -4.83 for R642H. The PROVEAN score is a value obtained from a computation analysis which inquires every amino acid position of all protein sequences in human and mouse and discriminate and predicts the impact of an amino acid substitution in the protein activity. Hence we were prompted to address the novel mutation as a very strong impact for the final folding and activity of NCC.

GS subjects are often heterozygous compound, specifically, to the onset of the disease they should carry two different mutations affecting two alleles of an autosome (1,18). A question that needs to be answered is what is the specific impact of each mutation in the final activity of the protein and the phenotype.

A mutation can affect the activity of a protein since the very beginning of its production. Nucleotide mutations in DNA can alter amino acids sequence with consequences in protein expression or function. Alterations can be missense and nonsense, insertion, deletion, duplication, frameshift mutations or repeat expansion.

The single amino acid replacement of glycine with aspartic acid at the position 394 was found to have a strong impact in terms of loss of function of the cotransporter.

Monogenic mutations are responsible for many kidney diseases and usually exhibit a genotype-phenotype correlation in single-gene disease of almost 100%. This means that a genetic investigation can predict the diagnosis of an inherited syndrome (73). Moreover, amino acid mutations can not only lead to mutated proteins, but also to its impaired trafficking, its endocytosis and its degradation (74). In fact the linear amino acids sequence is known to be translated into a three dimensional protein structure delineated by alpha-helices and β-sheets strands, which tends to arrange in a specific thermodynamically most stable conformation (69). An alternative amino acid sequence confers different properties of the residues, because of its altered electrical charge (e.g. positive or negative) or altered size. Glycine (G) is the smallest neutral non polar molecule while at physiological pH Aspartic (D) has acid characteristics with a negative charge in the lateral substituent. Therefore, the aforementioned mutation produces a substitution in the amino acid chain, with ensuing possible physical and chemical consequences on trafficking from the endoplasmic reticulum to the Golgi apparatus.

To prevent the expression of toxic peptides, the cell organizes complexes mechanisms as the recruiting of chaperones molecules that are able to denaturate misfolded proteins (75). In the kidney the enhanced endoplasmic reticulum-associated degradation (ERAD) acts triggering complexes of heat shock proteins Hsp70 and other components as ubiquitin-ligase, which are still unknown. By using a yeast model, Needham et al. showed that in Gitelman's syndrome there was a reduction of ER export due to NCC misfolding and that ERAD degradation influenced NCC turnover (76).

We found that in transfected HEK293 the G394D-NCC induces the production of a protein detectable at the western blot but with different characteristics form the NCC wild-type. Similar results were produce by De Jong et al., were they showed through de-glycosylation experiments, that the higher band resembled the fully glycosylated NCC (PMID 12039972). The absence of the fully glycosylated band in G394D-NCC suggests improper folding of the protein, albeit through mechanisms to be defined. The incorrect folding could led to lack of exposure of the extracellular loop with the two glycosylation sites across the 7^{th} and the 8^{th} domains. Moreover, the lack of glycosylation likely led to impaired trafficking of the protein to the membrane as shown by our immunohistochemistry experiments.

The Gly394Asp exchange is responsible for the correct folding of the protein by embedding a negative charge, which causes a disorder in the energy and in the physical properties of the structure. The resulted peptide is in turns recognized by the ERAD system, which therefore induces its early degradation.

Based on the data described in the study of De Jong, the ER-retained mutated NCC does not lack glycosylation, but is core-glycosylated and hence not fully glycosylated (77). Consistently, Hoover et al. showed that rat NCC has 404 and 424 asparagines N-linked sites critical for the glycosylation of the cotransporter (77-79). The central region, and particularly the 7th and 8th domains, seems to be highly specific for ion translocation and for thiazide–binding. Their external loop containing glycosylation sites are thus fundamental for the maturation of the protein and for the selectivity filter efficacy. A mutation in this position is therefore predicted to influence the activity of the protein (39,80). We used X. L. oocytes to better gain insights on the causes leading to an aberrant behavior of the protein. Since they do not express many proteins and thus do not develop a huge background, but their apparatus is ready to induce post-translational modifications, they are a well established tool to explore biochemical processes as protein signaling, transduction, phosphorylation and channels function (63,81).

Effect of gene mutation on glycosylation

By comparing in vitro the experiments in HEK293 cells and those in X.L. oocytes, we could confirm that wild-type proteins show at the western blot two bands: the core at 110 KDa and the glycosylated at 130 KDa, whereas the mutant cotransporter lack of the higher weight complex in accordance to the previous evidences (77,80). This finding could therefore explain the strong pathogenic impact of the novel mutation that is located in the 7th transmembrane fragment.

Effect of loss of glycosylation on protein

The immunohistochemical analysis provided evidence supporting the conclusion that the mutant protein triggers early ERAD in accordance with previous investigations (82,83). These experiments show that in wild-type injected oocytes, NCC reaches the plasma membrane, while, conversely, the mutants showed staining only in the intracellular area. The impaired folding results in an erroneous peptide, which is captured by the cytosolic control system, thus enhancing the retrieval for the degradation.

Effect of mutation on protein function

$^{22}Na^{+}$ uptake experiments endorsed the evidence that this mutation is causative of the pathology. When oocytes were incubated in the K^{+} free medium, these mutants were able to uptake only a small quantity of $^{22}Na^{+}$ compared to the wild-type (22,58% of total wild-type absorption). The addition of Metolazone, a thiazide-like drug, induced blockade of wild-type NCC, which resembled the quantity absorbed to the H_2O as vehicle injected. In G394D-NCC Metolazone did not reduced the basal absorption of indicating that G394D-NCC was not functional. The failure of the mutated cotransporter to uptake $^{22}Na^{+}$ as efficiently as the wild-type indicates the functional consequences of the mutation and establishes the inefficiency of G394D-NCC in terms proper folding, on trafficking leading to early protein degradation in ERAD.

Previously functional and expression analysis on oocytes described 3 different classes of NCC mutants in Gitelman's syndrome (7,77,84,85). Accordingly to those categories, Class I mutants are partially glycosylated but unable to uptake sodium. Class II mutants have uptake activity and are fully glycosylated but are only partially able to reach the surface. Class III mutants are glycosylated, expressed on the membranes, but unable to uptake sodium. This study show that the novel mutation entails an impaired glycosylation of the protein compared to the wild-type moreover, impaired trafficking at the membrane, with ensuing impaired the uptake. Hence, the novel mutation identified in this study reasonably could belong to a novel class of impaired proteins that are not glycosylated, can not reach the surface and do not function properly.

A recent review by Wang et al. elucidated that mutations have been identified spread all over the 26 exons but notwithstanding many attempts, most of them are too rare to allow identification of a correlation between genotype and phenotype (38). As it has been speculated that the position of the mutations and their outcome in terms of protein expression, glycosylation and phosphorylation could impact the severity of the syndrome our study add novel knowledge on the functional role of the 7^{th} -8^{th} transmembrane domains (86).

Occasionally GS phenotype is not correlated with a clear genotype, indeed some deep intronic mutations sometimes are not detectable but are translated in inclusion of cryptic exons in mRNA which arise in aberrant proteins (87,88). Moreover, the severity of the phenotype has been described to vary widely. According to Riveira-Munoz et al. observed one allele splicing mutation would lead to retained nonfunctional protein, and

would be prevalently present in the subgroup of patients screened harboring the most severe phenotype and in male subjects (80). The same observation was done by Lin et al., who described the heterogeneity of clinical phenotype in members of a family with identical mutations (89). The gender seems therefore to have a great influence, as studies with ovariectomized rats show that NCC plasma abundance is decreases and conversely, the treatment with estradiol restores its presence (90,91). This could be an explanation of the milder symptoms observed in GS female patients.

Notwithstanding an overactivation of the RAAS, GS patients have low blood pressure (92). Cruz et al. hypothesized that inherited mutations in genes involved in the control of the sodium reabsorption lower blood pressure (93). Given that salt wasting is the hallmark Gitelman's and Bartter's (BS) syndromes, Ji et al. investigated the presence of some genes causative of GS and BS, in the Framingham Heart Study (FHS) offspring cohort (4). They screened the Na-K-2Cl cotransporter gene (SLC12A1), the inward rectifier K^+ channel gene (KCNJ1) and the SLC12A3, observing the presence of functional mutations in one of the three genes with an incidence of 1/64 FHS members. They found that FHS individuals carrying those mutations had reduced blood pressure (4). These findings suggest the relevance of genetic mutations that are inherited among population with high blood pressure and that can even hide secondary hypertension.

Conclusion

This study shows that characterization of a novel mutation on NCC can lead not only to a better understanding of the molecular mechanisms causing GS but also to identification of functional role of the different molecular domains of the NCC.

ACKNOWLEDGMENTS

My gratitude goes to prof. Rossi, dr. Calò and last but not least to prof. Loffing for giving me the opportunity to plan and execute this very important project. My gratefulness goes also to all the Loffing's team (Dominique, Michéle, Sandra, Jan, David, Twinkle, Aga, Monique)
of the Institute of Anatomy at UZH, and dr. Pagnin, University of Padova, for giving me the excellent technical and formative support. I also thank prof. Zanotti, University of Padua, for kindly providing us a 3D structure of NCC mutated.

BIBLIOGRAPHY

(1) Knoers NV, Levtchenko EN. Gitelman syndrome. Orphanet J Rare Dis 2008 Jul 30;3:22-1172-3-22.

(2) Gitelman HJ, Graham JB, Welt LG. A new familial disorder characterized by hypokalemia and hypomagnesemia. Trans Assoc Am Physicians 1966;79:221-235.

(3) Favero M, Calo LA, Schiavon F, Punzi L. Miscellaneous non-inflammatory musculoskeletal conditions. Bartter's and Gitelman's diseases. Best Pract Res Clin Rheumatol 2011 Oct;25(5):637-648.

(4) Ji W, Foo JN, O'Roak BJ, Zhao H, Larson MG, Simon DB, et al. Rare independent mutations in renal salt handling genes contribute to blood pressure variation. Nat Genet 2008 May;40(5):592-599.

(5) Ravarotto V, Pagnin E, Fragasso A, Maiolino G, Calo LA. Angiotensin II and Cardiovascular-Renal Remodelling in Hypertension: Insights from a Human Model Opposite to Hypertension. High Blood Press Cardiovasc Prev 2015 Sep;22(3):215-223.

(6) Vargas-Poussou R, Dahan K, Kahila D, Venisse A, Riveira-Munoz E, Debaix H, et al. Spectrum of mutations in Gitelman syndrome. J Am Soc Nephrol 2011 Apr;22(4):693-703.

(7) Riveira-Munoz E, Chang Q, Bindels RJ, Devuyst O. Gitelman's syndrome: towards genotype-phenotype correlations? Pediatr Nephrol 2007 Mar;22(3):326-332.

(8) Naesens M, Steels P, Verberckmoes R, Vanrenterghem Y, Kuypers D. Bartter's and Gitelman's syndromes: from gene to clinic. Nephron Physiol 2004;96(3):p65-78.

(9) Watchorn E, McCance RA. Subacute magnesium deficiency in rats. Biochem J 1937 Aug;31(8):1379-1390.

(10) Spencer RW, Voyce MA. Familial hypokalaemia and hypomagnesaemia. A further family. Acta Paediatr Scand 1976 Jul;65(4):505-507.

(11) Zarraga Larrondo S, Vallo A, Gainza J, Muniz R, Garcia Erauzkin G, Lampreabe I. Familial hypokalemia-hypomagnesemia or Gitelman's syndrome: a further case. Nephron 1992;62(3):340-344.

(12) Hisakawa N, Yasuoka N, Itoh H, Takao T, Jinnouchi C, Nishiya K, et al. A case of Gitelman's syndrome with chondrocalcinosis. Endocr J 1998 Apr;45(2):261-267.

(13) Pachulski RT, Lopez F, Sharaf R. Gitelman's not-so-benign syndrome. N Engl J Med 2005 Aug 25;353(8):850-851.

(14) BARTTER FC, PRONOVE P, GILL JR,Jr, MACCARDLE RC. Hyperplasia of the juxtaglomerular complex with hyperaldosteronism and hypokalemic alkalosis. A new syndrome. Am J Med 1962 Dec;33:811-828.

(15) Scognamiglio R, Calo LA, Negut C, Coccato M, Mormino P, Pessina AC. Myocardial perfusion defects in Bartter and Gitelman syndromes. Eur J Clin Invest 2008 Dec;38(12):888-895.

(16) Bettinelli A, Tosetto C, Colussi G, Tommasini G, Edefonti A, Bianchetti MG. Electrocardiogram with prolonged QT interval in Gitelman disease. Kidney Int 2002 Aug;62(2):580-584.

(17) Simon DB, Karet FE, Hamdan JM, DiPietro A, Sanjad SA, Lifton RP. Bartter's syndrome, hypokalaemic alkalosis with hypercalciuria, is caused by mutations in the Na-K-2Cl cotransporter NKCC2. Nat Genet 1996 Jun;13(2):183-188.

(18) Simon DB, Karet FE, Rodriguez-Soriano J, Hamdan JH, DiPietro A, Trachtman H, et al. Genetic heterogeneity of Bartter's syndrome revealed by mutations in the K+ channel, ROMK. Nat Genet 1996 Oct;14(2):152-156.

(19) Simon DB, Bindra RS, Mansfield TA, Nelson-Williams C, Mendonca E, Stone R, et al. Mutations in the chloride channel gene, CLCNKB, cause Bartter's syndrome type III. Nat Genet 1997 Oct;17(2):171-178.

(20) Simon DB, Nelson-Williams C, Bia MJ, Ellison D, Karet FE, Molina AM, et al. Gitelman's variant of Bartter's syndrome, inherited hypokalaemic alkalosis, is caused by mutations in the thiazide-sensitive Na-Cl cotransporter. Nat Genet 1996 Jan;12(1):24-30.

(21) Kelly M, Semsarian C. Multiple Mutations in Genetic Cardiovascular Disease: A Marker of Disease Severity? Circulation: Cardiovascular Genetics 2009 April 01;2(2):182-190.

(22) Laghmani K, Beck BB, Yang SS, Seaayfan E, Wenzel A, Reusch B, et al. Polyhydramnios, Transient Antenatal Bartter's Syndrome, and MAGED2 Mutations. N Engl J Med 2016 May 12;374(19):1853-1863.

(23) Calo LA, Davis PA, Rossi GP. Understanding the mechanisms of angiotensin II signaling involved in hypertension and its long-term sequelae: insights from Bartter's and Gitelman's syndromes, human models of endogenous angiotensin II signaling antagonism. J Hypertens 2014 Nov;32(11):2109-19; discussion 2119.

(24) Fava C, Montagnana M, Rosberg L, Burri P, Almgren P, Jonsson A, et al. Subjects heterozygous for genetic loss of function of the thiazide-sensitive cotransporter have reduced blood pressure. Hum Mol Genet 2008 Feb 1;17(3):413-418.

(25) Clementi E. Role of nitric oxide and its intracellular signalling pathways in the control of Ca2+ homeostasis. Biochem Pharmacol 1998 Mar 15;55(6):713-718.

(26) Dzau VJ. Theodore Cooper Lecture: Tissue angiotensin and pathobiology of vascular disease: a unifying hypothesis. Hypertension 2001 Apr;37(4):1047-1052.

(27) Touyz RM, Schiffrin EL. Signal transduction mechanisms mediating the physiological and pathophysiological actions of angiotensin II in vascular smooth muscle cells. Pharmacol Rev 2000 Dec;52(4):639-672.

(28) Touyz RM. The role of angiotensin II in regulating vascular structural and functional changes in hypertension. Curr Hypertens Rep 2003 Apr;5(2):155-164.

(29) Calo L, Davis PA, Semplicini A. Reduced content of alpha subunit of Gq protein content in monocytes of Bartter and Gitelman syndromes: relationship with vascular hyporeactivity. Kidney Int 2002 Jan;61(1):353-354.

(30) Calo L, Ceolotto G, Milani M, Pagnin E, van den Heuvel LP, Sartori M, et al. Abnormalities of Gq-mediated cell signaling in Bartter and Gitelman syndromes. Kidney Int 2001 Sep;60(3):882-889.

(31) Calo L, Davis PA, Milani M, Cantaro S, Antonello A, Favaro S, et al. Increased endothelial nitric oxide synthase mRNA level in Bartter's and Gitelman's syndrome. Relationship to vascular reactivity. Clin Nephrol 1999 Jan;51(1):12-17.

(32) Calo L, Cantaro S, Calabro A, Piarulli F, Rizzolo M, Favaro S, et al. Endothelium-derived vasoactive substances in Bartter's syndrome. Angiology 1995 Oct;46(10):905-913.

(33) Calo LA, Puato M, Schiavo S, Zanardo M, Tirrito C, Pagnin E, et al. Absence of vascular remodelling in a high angiotensin-II state (Bartter's and Gitelman's syndromes): implications for angiotensin II signalling pathways. Nephrol Dial Transplant 2008 Sep;23(9):2804-2809.

(34) Calo L, Sartore G, Bassi A, Basso C, Bertocco S, Marin R, et al. Reduced susceptibility to oxidation of low-density lipoprotein in patients with overproduction of nitric oxide (Bartter's and Gitelman's syndrome). J Hypertens 1998 Jul;16(7):1001-1008.

(35) Calo LA, Savoia C, Davis PA, Pagnin E, Ravarotto V, Maiolino G. Relationship between NOX4 level and angiotensin II signaling in Gitelman's syndrome. Implications with hypertension. Int J Clin Exp Med 2015 May 15;8(5):7487-7496.

(36) Hediger MA, Romero MF, Peng JB, Rolfs A, Takanaga H, Bruford EA. The ABCs of solute carriers: physiological, pathological and therapeutic implications of human membrane transport proteinsIntroduction. Pflugers Arch 2004 Feb;447(5):465-468.

(37) Mastroianni N, Fusco MD, Zollo M, Arrigo G, Zuffardi O, Bettinelli A, et al. Molecular Cloning, Expression Pattern, and Chromosomal Localization of the Human Na–Cl Thiazide-Sensitive Cotransporter (SLC12A3). Genomics 1996 8/1;35(3):486-493.

(38) Wang L, Dong C, Xi YG, Su X. Thiazide-sensitive Na+-Cl- cotransporter: genetic polymorphisms and human diseases. Acta Biochim Biophys Sin (Shanghai) 2015 May;47(5):325-334.

(39) Moreno E, Cristobal PS, Rivera M, Vazquez N, Bobadilla NA, Gamba G. Affinity-defining domains in the Na-Cl cotransporter: a different location for Cl- and thiazide binding. J Biol Chem 2006 Jun 23;281(25):17266-17275.

(40) Plotkin MD, Kaplan MR, Verlander JW, Lee W, Brown D, Poch E, et al. Localization of the thiazide sensitive Na-Cl cotransporter, rTSC1, in the rat kidney. Kidney Int 1996 June 1996;50(1):174-183.

(41) Ellison DH, Velazquez H, Wright FS. Thiazide-sensitive sodium chloride cotransport in early distal tubule. Am J Physiol Renal Physiol 1987 American Physiological Society;253(3):F546-F554.

(42) Poulsen SB, Christensen BM. Long-term aldosterone administration increases renal Na+-Cl- cotransporter abundance in late distal convoluted tubule. Am J Physiol Renal Physiol 2016 Oct 12:ajprenal.00352.2016.

(43) Loffing J, Kaissling B. Sodium and calcium transport pathways along the mammalian distal nephron: from rabbit to human. Am J Physiol Renal Physiol 2003 Apr;284(4):F628-43.

(44) Crayen ML, Thoenes W. Architecture and cell structures in the distal nephron of the rat kidney. Cytobiologie 1978 Jun;17(1):197-211.

(45) Biner HL, Arpin-Bott MP, Loffing J, Wang X, Knepper M, Hebert SC, et al. Human cortical distal nephron: distribution of electrolyte and water transport pathways. J Am Soc Nephrol 2002 Apr;13(4):836-847.

(46) Loffing J, Pietri L, Aregger F, Bloch-Faure M, Ziegler U, Meneton P, et al. Differential subcellular localization of ENaC subunits in mouse kidney in response to high- and low-Na diets. Am J Physiol Renal Physiol 2000 Aug;279(2):F252-8.

(47) Schmitt R, Ellison DH, Farman N, Rossier BC, Reilly RF, Reeves WB, et al. Developmental expression of sodium entry pathways in rat nephron. Am J Physiol 1999 Mar;276(3 Pt 2):F367-81.

(48) Loffing J, Loffing-Cueni D, Hegyi I, Kaplan MR, Hebert SC, Le Hir M, et al. Thiazide treatment of rats provokes apoptosis in distal tubule cells. Kidney Int 1996 Oct;50(4):1180-1190.

(49) Loffing J, Korbmacher C. Regulated sodium transport in the renal connecting tubule (CNT) via the epithelial sodium channel (ENaC). Pflugers Arch 2009 May;458(1):111-135.

(50) Arroyo JP, Ronzaud C, Lagnaz D, Staub O, Gamba G. Aldosterone paradox: differential regulation of ion transport in distal nephron. Physiology (Bethesda) 2011 Apr;26(2):115-123.

(51) Hunter RW, Ivy JR, Flatman PW, Kenyon CJ, Craigie E, Mullins LJ, et al. Hypertrophy in the Distal Convoluted Tubule of an 11beta-Hydroxysteroid Dehydrogenase Type 2 Knockout Model. J Am Soc Nephrol 2015 Jul;26(7):1537-1548.

(52) Bostanjoglo M, Reeves WB, Reilly RF, Velazquez H, Robertson N, Litwack G, et al. 11Beta-hydroxysteroid dehydrogenase, mineralocorticoid receptor, and thiazide-sensitive Na-Cl cotransporter expression by distal tubules. J Am Soc Nephrol 1998 Aug;9(8):1347-1358.

(53) Reilly RF, Ellison DH. Mammalian distal tubule: physiology, pathophysiology, and molecular anatomy. Physiol Rev 2000 Jan;80(1):277-313.

(54) Kim TK, Eberwine JH. Mammalian cell transfection: the present and the future. Anal Bioanal Chem 2010 Aug;397(8):3173-3178.

(55) Woods NB, Muessig A, Schmidt M, Flygare J, Olsson K, Salmon P, et al. Lentiviral vector transduction of NOD/SCID repopulating cells results in multiple vector integrations per transduced cell: risk of insertional mutagenesis. Blood 2003 Feb 15;101(4):1284-1289.

(56) Washbourne P, McAllister AK. Techniques for gene transfer into neurons. Curr Opin Neurobiol 2002 10/1;12(5):566-573.

(57) Mehier-Humbert S, Guy RH. Physical methods for gene transfer: improving the kinetics of gene delivery into cells. Adv Drug Deliv Rev 2005 Apr 5;57(5):733-753.

(58) Graham FL, Smiley J, Russell WC, Nairn R. Characteristics of a human cell line transformed by DNA from human adenovirus type 5. J Gen Virol 1977 Jul;36(1):59-74.

(59) Harland RM, Grainger RM. Xenopus research: metamorphosed by genetics and genomics. Trends Genet 2011 Dec;27(12):507-515.

(60) Broer S. Xenopus laevis Oocytes. Methods Mol Biol 2010;637:295-310.

(61) Angerer LM, Angerer RC. Animal-vegetal axis patterning mechanisms in the early sea urchin embryo. Dev Biol 2000 Feb 1;218(1):1-12.

(62) Sive HL, Grainger RM, Harland RM. Defolliculation of Xenopus oocytes. Cold Spring Harb Protoc 2010 Dec 1;2010(12):pdb.prot5535.

(63) Cristofori-Armstrong B, Soh MS, Talwar S, Brown DL, Griffin JD, Dekan Z, et al. Xenopus borealis as an alternative source of oocytes for biophysical and pharmacological studies of neuronal ion channels. Sci Rep 2015 Oct 6;5:14763.

(64) Gromiha MM, An J, Kono H, Oobatake M, Uedaira H, Prabakaran P, et al. ProTherm, version 2.0: thermodynamic database for proteins and mutants. Nucleic Acids Res 2000 Jan 1;28(1):283-285.

(65) Adzhubei IA, Schmidt S, Peshkin L, Ramensky VE, Gerasimova A, Bork P, et al. A method and server for predicting damaging missense mutations. Nat Methods 2010 Apr;7(4):248-249.

(66) Capriotti E, Fariselli P, Casadio R. I-Mutant2.0: predicting stability changes upon mutation from the protein sequence or structure. Nucleic Acids Res 2005 Jul 1;33(Web Server issue):W306-10.

(67) Mastroberardino L, Spindler B, Forster I, Loffing J, Assandri R, May A, et al. Ras pathway activates epithelial Na+ channel and decreases its surface expression in Xenopus oocytes. Mol Biol Cell 1998 Dec;9(12):3417-3427.

(68) Monroy A, Plata C, Hebert SC, Gamba G. Characterization of the thiazide-sensitive Na(+)-Cl(-) cotransporter: a new model for ions and diuretics interaction. Am J Physiol Renal Physiol 2000 Jul;279(1):F161-9.

(69) Anfinsen CB. The formation and stabilization of protein structure. Biochem J 1972 Jul;128(4):737-749.

(70) Hebert SC, Mount DB, Gamba G. Molecular physiology of cation-coupled Cl- cotransport: the SLC12 family. Pflugers Arch 2004 Feb;447(5):580-593.

(71) Hartmann AM, Tesch D, Nothwang HG, Bininda-Emonds OR. Evolution of the cation chloride cotransporter family: ancient origins, gene losses, and subfunctionalization through duplication. Mol Biol Evol 2014 Feb;31(2):434-447.

(72) Gamba G. Molecular physiology and pathophysiology of electroneutral cation-chloride cotransporters. Physiol Rev 2005 Apr;85(2):423-493.

(73) Hildebrandt F. Genetic kidney diseases. Lancet 2010 Apr 10;375(9722):1287-1295.

(74) Schaeffer C, Creatore A, Rampoldi L. Protein trafficking defects in inherited kidney diseases. Nephrol Dial Transplant 2014 Sep;29 Suppl 4:iv33-44.

(75) Wang M, Kaufman RJ. Protein misfolding in the endoplasmic reticulum as a conduit to human disease. Nature 2016 Jan 21;529(7586):326-335.

(76) Needham PG, Mikoluk K, Dhakarwal P, Khadem S, Snyder AC, Subramanya AR, et al. The thiazide-sensitive NaCl cotransporter is targeted for chaperone-dependent endoplasmic reticulum-associated degradation. J Biol Chem 2011 Dec 23;286(51):43611-43621.

(77) De Jong JC, Van Der Vliet WA, Van Den Heuvel LP, Willems PH, Knoers NV, Bindels RJ. Functional expression of mutations in the human NaCl cotransporter: evidence for impaired routing mechanisms in Gitelman's syndrome. J Am Soc Nephrol 2002 Jun;13(6):1442-1448.

(78) de Jong JC, Willems PH, Mooren FJ, van den Heuvel LP, Knoers NV, Bindels RJ. The structural unit of the thiazide-sensitive NaCl cotransporter is a homodimer. J Biol Chem 2003 Jul 4;278(27):24302-24307.

(79) Hoover RS, Poch E, Monroy A, Vazquez N, Nishio T, Gamba G, et al. N-Glycosylation at two sites critically alters thiazide binding and activity of the rat thiazide-sensitive Na(+):Cl(-) cotransporter. J Am Soc Nephrol 2003 Feb;14(2):271-282.

(80) Riveira-Munoz E, Chang Q, Godefroid N, Hoenderop JG, Bindels RJ, Dahan K, et al. Transcriptional and functional analyses of SLC12A3 mutations: new clues for the pathogenesis of Gitelman syndrome. J Am Soc Nephrol 2007 Apr;18(4):1271-1283.

(81) Wheeler GN, Brandli AW. Simple vertebrate models for chemical genetics and drug discovery screens: lessons from zebrafish and Xenopus. Dev Dyn 2009 Jun;238(6):1287-1308.

(82) Kuznetsov G, Nigam SK. Folding of secretory and membrane proteins. N Engl J Med 1998 Dec 3;339(23):1688-1695.

(83) Gregersen N, Bolund L, Bross P. Protein misfolding, aggregation, and degradation in disease. Mol Biotechnol 2005 Oct;31(2):141-150.

(84) Kunchaparty S, Palcso M, Berkman J, Velazquez H, Desir GV, Bernstein P, et al. Defective processing and expression of thiazide-sensitive Na-Cl cotransporter as a cause of Gitelman's syndrome. Am J Physiol 1999 Oct;277(4 Pt 2):F643-9.

(85) Sabath E, Meade P, Berkman J, de los Heros P, Moreno E, Bobadilla NA, et al. Pathophysiology of functional mutations of the thiazide-sensitive Na-Cl cotransporter in Gitelman disease. Am J Physiol Renal Physiol 2004 Aug;287(2):F195-203.

(86) Tseng MH, Yang SS, Hsu YJ, Fang YW, Wu CJ, Tsai JD, et al. Genotype, phenotype, and follow-up in Taiwanese patients with salt-losing tubulopathy associated with SLC12A3 mutation. J Clin Endocrinol Metab 2012 Aug;97(8):E1478-82.

(87) Lo YF, Nozu K, Iijima K, Morishita T, Huang CC, Yang SS, et al. Recurrent deep intronic mutations in the SLC12A3 gene responsible for Gitelman's syndrome. Clin J Am Soc Nephrol 2011 Mar;6(3):630-639.

(88) Nozu K, Iijima K, Nozu Y, Ikegami E, Imai T, Fu XJ, et al. A deep intronic mutation in the SLC12A3 gene leads to Gitelman syndrome. Pediatr Res 2009 Nov;66(5):590-593.

(89) Lin SH, Cheng NL, Hsu YJ, Halperin ML. Intrafamilial phenotype variability in patients with Gitelman syndrome having the same mutations in their thiazide-sensitive sodium/chloride cotransporter. Am J Kidney Dis 2004 Feb;43(2):304-312.

(90) Verlander JW, Tran TM, Zhang L, Kaplan MR, Hebert SC. Estradiol enhances thiazide-sensitive NaCl cotransporter density in the apical plasma membrane of the distal convoluted tubule in ovariectomized rats. J Clin Invest 1998 Apr 15;101(8):1661-1669.

(91) Rojas-Vega L, Gamba G. Mini-review: regulation of the renal NaCl cotransporter by hormones. Am J Physiol Renal Physiol 2016 Jan 1;310(1):F10-4.

(92) Calo LA, Schiavo S, Davis PA, Pagnin E, Mormino P, D'Angelo A, et al. Angiotensin II signaling via type 2 receptors in a human model of vascular hyporeactivity: implications for hypertension. J Hypertens 2010 Jan;28(1):111-118.

(93) Cruz DN, Simon DB, Nelson-Williams C, Farhi A, Finberg K, Burleson L, et al. Mutations in the Na-Cl cotransporter reduce blood pressure in humans. Hypertension 2001 Jun;37(6):1458-1464.